Eukaryotic biodiversity and ecological networks from the surface to the mesopelagic in the Northwest Atlantic Slope Water

Nina Yang[1,2], Elizabeth A. Allan[3], Sarah E. Stover[1†], Benjamin D. Grassian[1,4‡], Heidi M. Sosik[1], Joel K. Llopiz[1], Annette F. Govindarajan[1]

[1]Department of Biology, Woods Hole Oceanographic Institution, Woods Hole, MA, USA

[2]Marine Policy Center, Woods Hole Oceanographic Institution, Woods Hole, MA, USA

[3]School of Marine and Environmental Affairs, University of Washington, Seattle, Washington, USA

[4]Department of Applied Ocean Physics and Engineering, Woods Hole Oceanographic Institution, Woods Hole, MA, USA

Correspondence: Nina Yang, nina.yang@whoi.edu

[†]**Present Address:** Graduate School of Biology, University of Vermont, Burlington, Vermont, USA

[‡]**Present Address**: Graduate School of Oceanography, University of Rhode Island, Narragansett, RI, USA

1. ABSTRACT

The diversity and interactions among mesopelagic organisms are difficult to study and as a result, are insufficiently unaccounted for in food web and biogeochemical models. This knowledge gap hinders our ability to model and forecast ecosystem function and formulate effective policies for conservation and management in the face of growing interest in exploiting midwater living resources. We used multi-marker metabarcoding of environmental DNA (eDNA) samples collected from Northwest Atlantic Slope Water to resolve patterns of eukaryotic community composition spanning taxonomically across protists (microbial eukaryotes), invertebrates, and vertebrates and vertically from the ocean surface to the base of the mesopelagic zone. With statistical network analyses, we explored cross-kingdom associations including putative trophic dynamics such as food web interactions and evaluated network robustness to biodiversity loss. We found depth-specific communities of distinct protist, invertebrate, and vertebrate assemblages. Ecological networks for the epipelagic, upper mesopelagic, and lower mesopelagic suggest that protists are keystone taxa and important mediators of trophic interactions; they increase network complexity and contribute to network stability. We also identified metazoans including copepods, gelatinous taxa (cnidarians, tunicates), and mesopelagic fish as important components of network interactions. Our study demonstrates a holistic approach to generate insights on mesopelagic biodiversity and implications for ecosystem resilience that can inform ocean governance.

2. INTRODUCTION

In the vast mesopelagic region of the ocean from the base of the sunlit zone to 1000 m deep (Buesseler et al., 2020), diverse ecological communities underpin ecosystem function and critical ecosystem services (Oliver et al., 2015; Sala et al., 2021; Nauta and De Domenico, 2024). A wide variety of life, from microscopic phytoplankton to apex predators, comprise complex food webs that support commercially and ecologically important species including sharks, tuna, and billfish (Braun et al., 2023; Iglesias et al., 2023; Willis et al., 2025). In addition, mesopelagic biodiversity play an important role in climate regulation by carrying out biogeochemical processes that determine carbon flux into deeper waters and thus, its long-term sequestration (e.g., 10-1000 years) (Herndl and Reinthaler, 2013; Mazuecos et al., 2015; Cavan et al., 2019; Nguyen et al., 2022).

The mesopelagic zone is intrinsically linked to the surface ocean or epipelagic zone (< 200 m) where phytoplankton harness energy from the sun to convert carbon dioxide into organic carbon. Zooplankton grazing and senescence of primary production can export organic carbon out of the epipelagic, providing a food source for life in the deep ocean (Cawley et al., 2021; Hemsley et al., 2023) and contributing to the largest reservoir of organic carbon on earth (Arístegui et al., 2009). In addition, animals that migrate from the depths to feed at the surface actively transport carbon into deeper waters through diel vertical migration (DVM) behaviors, further demonstrating the interconnected nature of the epipelagic and mesopelagic ocean (Robinson et al., 2010; Davison et al., 2013; Thibault et al., 2025).

Despite the recognized importance of the deep sea, biodiversity and ecological studies have primarily focused on coastal or epipelagic ecosystems, leaving the mesopelagic both undersampled and understudied (Webb et al., 2010; St. John et al., 2016). These knowledge gaps are largely driven by challenges associated with accessing and sampling a vast ecosystem that spans considerable horizontal and vertical spatial scales (Sutton et al., 2017). Difficulty in acquiring logistical resources and expertise for deep sea exploration and research are also major

contributing factors (Tolochko and Vadrot, 2021; Amon et al., 2022b). Furthermore, many studies focus on specific groups of organisms in isolation, such as those exclusively examining microbes or metazoans (Yang et al., 2024), which skews our understanding of biodiversity, ecological interactions, and functional roles.

Growing interest in mesopelagic fisheries for aquaculture and nutraceuticals (Martin et al., 2020; Bisson et al., 2023), deep sea mining activities (Drazen et al., 2020; Amon et al., 2022a; Dowd et al., 2025), and marine carbon dioxide removal efforts (Hernández-León, 2023; Oschlies et al., 2025) presents increasing pressures on the mesopelagic and its ecosystem services, including overexploitation and habitat destruction. In the face of these anthropogenic pressures, limited data present significant challenges for effective ocean governance of deep pelagic ecosystems, including conservation, resource management, and environmental impact assessments.

In the last decade, environmental DNA (eDNA) approaches have emerged as a reliable and non-invasive solution to survey biodiversity (McClenaghan et al., 2020; Chavez et al., 2021; Holman et al., 2021; Yeh and Fuhrman, 2022; Govindarajan et al., 2023a; Dan et al., 2024). With eDNA, organisms across all domains of life can be detected from a single water sample by targeting multiple marker genes (Amaral-Zettler et al., 2009; Miya et al., 2015), making eDNA approaches ideal for large-scale biomonitoring across varied spatiotemporal scales (Deiner et al., 2017; Gold et al., 2021, 2022; Blancher et al., 2022; De Brauwer et al., 2023; Thomsen et al., 2024). However, few multi-marker metabarcoding studies have been conducted in deep pelagic ecosystems and existing studies tend to emphasize organismal diversity and distribution rather than interactions among taxa (Giner et al., 2020; Laroche et al., 2020a; Govindarajan et al., 2021; Holman et al., 2021; Govindarajan et al., 2023b). A more holistic approach would facilitate our ability to effectively understand how community composition and organismal interactions across eukaryotic taxa influence crucial ecosystem processes. For example, recent studies have employed multi-marker metabarcoding approaches to resolve diversity patterns from prokaryotes

to top predators (Djurhuus et al., 2020; Holman et al., 2021). Using statistical and network analyses, these studies also documented key predator-prey interactions, identified potential keystone taxa, and uncovered unexplored trophic connections. Collectively, these insights provide necessary context for ecosystem health and may serve as important indicators for ecosystem function in a changing ocean.

We applied an eDNA metabarcoding approach with two gene markers to investigate patterns of eukaryotic biodiversity and their interactions to better understand ecosystem structure of the epipelagic and mesopelagic zones in the Northwest Atlantic Slope Water region. We calculated diversity indices to determine depth-specific biodiversity patterns. We then performed covariance network analyses on multi-marker metabarcoding data, constructing depth-specific networks for metazoans (invertebrates and vertebrates), protists, and all taxa combined across the epipelagic (10 m, 100 m), upper mesopelagic (300 m, 500 m), and lower mesopelagic (800 m, 1000 m) depth zones. Network topologies revealed depth-specific trends of network complexity determined by the total number of nodes (amplicon sequence variants or ASVs), edges (interactions or links), and link density (edge-to-node ratio) (Landi et al., 2018). We explored the influence of complexity across depth zones on network stability, determined by sequentially removing ASVs from the networks (node connectivity and robustness) and edges (edge connectivity) (Iyer et al., 2013; Tipton et al., 2018). These analyses provide a survey of water column biodiversity and reveal insights on the role of keystone taxa and their potential interactions in food webs and ecosystem resilience.

3. MATERIALS & METHODS

3. 1. Sample Collection

Bulk water samples were collected in Northwest Atlantic Slope Water off the coast of New Jersey, eastern United States in March 2020 on the *R/V* Armstrong (AR43) at six discrete depths (10 m, 100 m, 300 m, 500 m, 800 m, and 1000 m) at three sampling stations (Figure 1,

Supplementary Table S1). Sampling spanned surface depths to the base of the mesopelagic and included the deep scattering layer (~500 m) as determined by a broadband Simrad EK80 split beam echosounder system on the *R/V* Armstrong (Supplementary Figure S1, Supplementary Methods). Water was collected with a 24-Niskin CTD rosette across three casts at sampling sites with similar water column characteristics (Figure 1). Two casts (001 and 007) were collected at midnight while cast 002 was collected at mid-day. At each depth, four replicates were collected for a total of 72 samples. For each sample, ~5 L of water was pumped through sterile 0.2 µm PES Sterivex (MilliporeSigma, Burlington, MA, USA) filters, sealed with Luer lock caps, and stored at -80°C. Sample collection carboys and filtration tubing were bleach-sterilized and rinsed with Milli-Q water prior to filtration with a Masterflex L/S peristaltic pump system following established protocols (Govindarajan et al., 2021, 2022).

The AR43 expedition coincided with high densities of the salp *Salpa aspera*, gelatinous zooplankton that are known to periodically "bloom" in the Northwest Atlantic Slope Water (Wiebe et al., 1979; Madin et al., 2006). From analysis of in situ high speed (15 Hz) image data, we estimated densities of 5-10 individuals m^{-3} in surface waters at night (Supplementary Figure S2, Supplementary Methods), which are in the typical range for bloom densities (e.g., 3.5 individuals m^{-3} and higher) (Groeneveld et al., 2020).

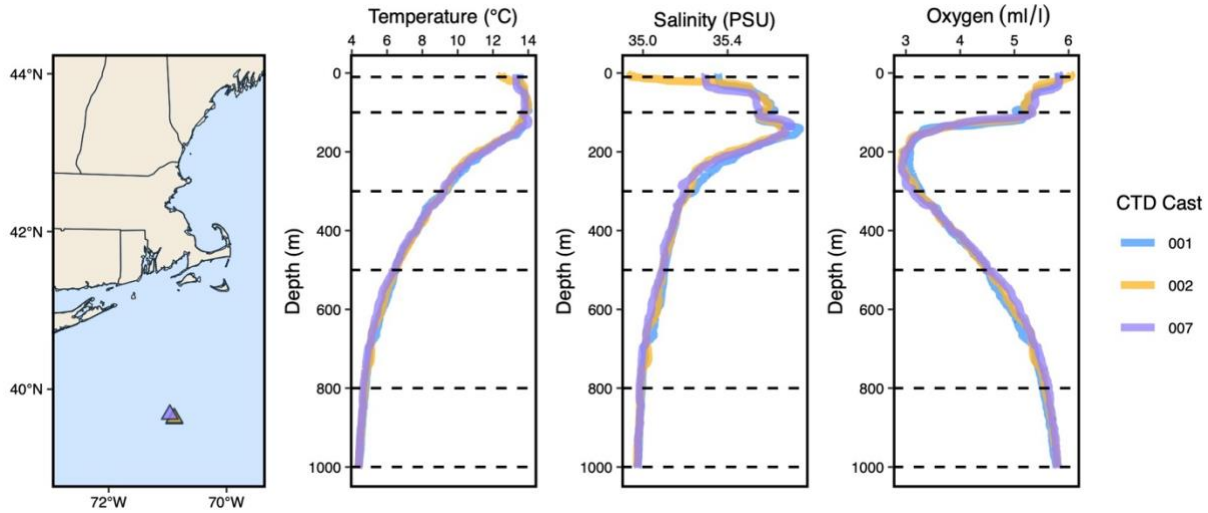

Figure 1. Sampling location and CTD profiles for eDNA collection. Temperature, salinity, and oxygen profiles for each CTD cast (001, 002, and 007) where eDNA samples were collected are shown. Dashed black lines indicate the depths where samples were collected (10 m, 100 m, 300 m, 500 m, 800 m, and 1000 m). Coordinates for sampling sites are provided in Supplementary Table S1.

3.2. DNA Extractions and PCR

DNA was extracted with a Qiagen DNEasy Blood & Tissue extraction kit (Qiagen, Germantown, MD, USA) following manufacturer's protocols with modifications for Sterivex filters (Govindarajan et al., 2021). Extracted DNA was stored at -20°C prior to metabarcoding. All samples were metabarcoded for portions of the 18S and 12S rRNA genes (see below), except for one sample collected on CTD cast 007 at 1000 m which did not have enough DNA template for 12S rRNA metabarcoding. All lab surfaces and equipment were cleaned with a 10% sodium hypochlorite solution (household bleach) and extractions were performed in a dedicated laboratory space away from sources of concentrated DNA such as post-PCR or tissue samples.

The 18S V9 hypervariable region was amplified using the 1380F/1510R primer set with CS1/CS2 Fluidigm adapters and following a two-step PCR protocol (Amaral-Zettler et al., 2009; Govindarajan et al., 2021). The initial PCR cycling program began with a denaturation step at 95°C for 3 min, 25 cycles at 95°C for 30 sec, 55°C for 30 sec, and 72°C for 30 sec, followed by an elongation step at 72°C for 5 min. PCR reactions (25 µl) consisted of 2.5 µl of DNA template,

155 0.5 µl of each primer, 12.5 µl of 2x KAPA HiFi HotStart ReadyMix (Kapa Biosystems; Wilmington,
156 MA, USA), and 9 µl of molecular-grade water. Duplicate PCR reactions were run for each sample,
157 pooled, and sent to the Genome Research Core at the University of Illinois at Chicago (UIC) to
158 complete a second PCR amplification to add unique tags using MyTaq HS 2X Master Mix and the
159 Access Array Barcode Library for Illumina (Fluidigm, South San Francisco, CA, USA). The PCR
160 cycling program was as follows: 95°C for 5 min followed by 18 cycles of 95°C for 30 sec, 60°C for
161 30 sec, 72°C for 30 sec, and 72°C for 7 min. Amplicon libraries were purified using AMPure XP
162 beads (Beckman Coulter, Indianapolis, IN, USA). Amplicon sequencing with a targeted
163 sequencing depth of 100000 reads per sample was done on an Illumina MiSeq (2x250 bp)
164 (Govindarajan et al., 2022).

165 The hypervariable 12S region of the mitochondrial rRNA gene was amplified using MiFish
166 primers (Miya et al., 2015) appended with Illumina adapter overhang nucleotide sequences and
167 a modified two-step PCR protocol with a touch-down PCR program for the first PCR (Pitz et al.,
168 2020). The initial PCR cycling program began with a denaturation step at 95°C for 15 min; 13
169 cycles of 94°C for 30 sec, 69.5°C for 30 sec (decreasing 1.5°C with each cycle), and 72°C for 90
170 sec; 25 cycles of 94°C for 30 sec, 50°C for 30 sec, and 72°C for 45 sec; followed by an elongation
171 step at 72 °C for 10 min. PCR reactions (25 µl) consisted of 2.5 µl of DNA template, 1 µl of each
172 primer, 12.5 µl of 2x KAPA HiFi HotStart ReadyMix, and 8 µl of molecular-grade water. Duplicate
173 PCR products were pooled and sent to the Center for Genome Innovation at the University of
174 Connecticut for size selection, a second round of PCR, and sequencing. Amplicons from the
175 pooled PCR products were visualized with the Agilent 4200 TapeStation electrophoresis system
176 using the High Sensitivity DNA D1000 assay (Agilent Technologies, Santa Clara, CA). Size-
177 selection for targeted amplicons (215bp-335bp) was conducted using the Sage Science
178 PippinPrep HT gel cassette (2% Agarose, PippinHT). Illumina barcodes were added to each
179 amplicon using a second PCR amplification. The PCR cycling program was as follows: 95°C for
180 3 min followed by 12 cycles of 95°C for 15 sec, 60°C for 30 sec, and 72°C for 90 sec. Amplicon

181 libraries were purified using AMPure XP beads and assessed for quality and adapter dimer
182 content on the Agilent 4200 TapeStation using a D1000 assay. Amplicon sequencing with a
183 targeted sequencing depth of 100000 reads per sample was done on an Illumina MiSeq
184 (2x250bp) with 20–30% PhiX added (Illumina, San Diego, CA).

185 For both 18S and 12S primer sets, PCR runs included field controls of filtered Milli-Q water
186 (1 L for each CTD cast) as well as PCR negative (without DNA template) and positive controls.
187 The PCR positive control was included to determine the quality of sequencing results and
188 consisted of previously extracted 1ng/µl sample of *Fundulus heteroclitus*, an estuarine fish that
189 would not be found in the environmental samples.

190

191 **3.3 Multi-marker metabarcoding bioinformatics**

192 Demultiplexed sequencing reads were imported into and processed in QIIME 2 with
193 default settings (v2022.11.1) (Bolyen et al., 2019). Adapters and primers were trimmed from the
194 reads with Cutadapt (Martin, 2011). Reads were quality-filtered, trimmed to the primer region 120
195 bp (18S) and 150 bp (12S), denoised, and merged into ASVs with DADA2 (Callahan et al., 2016).
196 ASVs represent exact biological sequences that can be distinguished by as little as one nucleotide
197 (Callahan et al., 2017). For both gene markers, taxonomy was assigned by a naïve Bayes
198 classifier at an 80% confidence threshold (Pedregosa et al., 2011); the classifier was trained on
199 reference databases curated and evaluated with the REference Sequence annotation and
200 CuRatIon Pipeline (RESCRIPt) QIIME 2 plugin (Robeson et al., 2021).

201 The 18S sequencing reads were annotated with two different databases: one for protists
202 and one for metazoans. The protist (18S) classifier was trained with the Protistan Ribosomal
203 Reference (PR2) database (v5.0.1) (Guillou et al., 2013) that was updated with 9 taxonomic levels
204 including the replacement of kingdom with domain and the addition of a new subdivision level.
205 The metazoan (18S) classifier was trained with the SILVA SSURef_NR99 (v138.1) database
206 (Pruesse et al., 2007; Quast et al., 2013). A new 12S classifier was created by combining a

207 custom reference database of 12S sequences for 80 species of mesopelagic fish from the
208 Northwest Atlantic (Govindarajan et al., 2023b) with the MetaZooGene database (v2023-m07-15)
209 in Mode-A (most inclusive option) for vertebrates (O'Brien et al., 2024). For 18S sequences,
210 taxonomy assignments were first assigned with PR2 and protist sequences were selected as the
211 subset where phylum was not classified as "Metazoa". This subset will be referred to as the protist
212 dataset. Sequences where phylum was classified as "Metazoa" were subsequently classified with
213 the SILVA-based classifier. Metazoan 18S reads were classified predominantly as invertebrate
214 taxa and will be referred to as the invertebrate dataset (Govindarajan et al., 2021). Likewise,
215 metazoan 12S reads were classified as vertebrates (mainly fishes) and will be referred to as the
216 vertebrate dataset. For downstream bioinformatic and statistical analyses, the 18S reads were
217 processed separately as two individual datasets representing protist and invertebrate reads, while
218 12S reads represented the standalone vertebrate dataset.

219 After taxonomic classification, 142 of 399 invertebrate ASVs remained unassigned at the
220 phylum level or were unassigned sequences from the phylum Arthropoda, which represented
221 18.4% of all sequences in the invertebrate dataset. Of those 142 ASVs, one ASV represented
222 ~13% of invertebrate reads and comprised of ~48% of reads at 100 m (Supplementary Figure
223 S3A). These unassigned sequences were manually classified with Geneious Prime 2025.0.3 with
224 a BLAST search and NCBI's new BLAST core nucleotide database (core_nt). The top match was
225 selected from the assigned grade score at a 95% cut-off. This approach annotated 67 of the 142
226 unassigned invertebrate ASVs, which reduced the total number of unassigned reads to 0.35%.
227 Most unassigned reads were classified to Order Calanoida (calanoid copepods). Similarly, 345 of
228 677 vertebrate ASVs remained unassigned with > 80% of ASVs classified as Unassigned
229 Actinopterygii (ray-finned fishes). Altogether, unassigned ASVs comprised 12.9% of reads.
230 Following the BLAST process described for invertebrates, 117 vertebrate ASVs were successfully
231 classified, reducing the unassigned read percentage to ~1% (Supplementary Figure S3B).

232 Taxonomy, ASV count, and metadata files were imported into R (v4.3.2) with qiime2R
233 (v0.99.6) (https://github.com/jbisanz/qiime2R) and merged with phyloseq (v1.46.0) (McMurdie
234 and Holmes, 2013) to generate phyloseq objects for protists, invertebrates, and vertebrates.
235 Potential contaminants were identified and removed with the R package decontam and a
236 conservative threshold of 0.5, which identifies all sequences more prevalent in negative controls
237 than samples as contaminants (Davis et al., 2018). In total, decontam identified and removed 44
238 protist, 19 invertebrate, and 17 vertebrate ASVs. Additional decontamination of the datasets was
239 conducted manually and detailed in Supplementary Methods. Sequencing thresholds were
240 selected to remove low read-depth outliers (Schloss, 2024a) such that samples with less than
241 15000 reads (protists), 6000 reads (invertebrates), and 3000 reads (vertebrates) were removed,
242 resulting in 69 samples (protists), 70 samples (invertebrates), and 61 samples (vertebrates) out
243 of 72 total samples (Supplementary Figure S4).
244
245 **3.4 Community Ecology Analyses**
246 Alpha diversity indices (richness, Shannon Index, evenness) were calculated from a
247 rarefaction approach with iterative subsampling (1000 iterations) and a subsampling threshold
248 (Schloss, 2024a) determined by the minimum read count of 27865 (protists), 6076 (invertebrates),
249 and 3183 (vertebrates) in the sample set (Schloss, 2024b). Diversity indices reflect the mean
250 index value for each depth after rarefaction and statistical significance was computed by one-way
251 ANOVA with Tukey's HSD post-hoc analysis (p value < 0.05).
252 Depth-specific community composition was assessed with principal component analyses
253 conducted with the rda function in vegan v2.6.4 (Oksanen et al., 2022) on centered log-ratio (CLR)
254 transformed ASV counts (Aitchson, 1986; Quinn et al., 2018; Coenen et al., 2020). Zero-value
255 data were replaced with the "const" method which replaces zeros with 65% of the next lowest
256 value (Bastiaanssen et al., 2022). Statistical significance was assessed with permutational
257 multivariate analysis of variance (PERMANOVA) with the adonis2 function in vegan on Euclidean

distance matrices calculated from CLR-transformed data (i.e., Aitchison distance). Pairwise comparisons were conducted with the pairwise.adonis2 function from the pairwiseAdonis package v0.4 (Arbizu, 2020).

ASVs were grouped into relevant taxonomic groups for taxa bar plots to show the proportion of ASV composition and relative abundance. UpSet plots were used to visualize ASV overlap across depths, with a matrix format that shows which ASVs are shared or unique to specific depths. Taxa with low relative abundance (< 1%) were grouped to streamline visualizations with additional details provided in Supplementary Materials (Supplementary Tables S2-S4). ASV accumulation curves were generated with the specaccum function in vegan v2.6.8 with the “random” method, which randomizes sample order and averages ASV richness across 999 permutations to show how ASV richness increases with sampling effort.

3.5 Network Analyses

Network analysis from Sparse InversE Covariance Estimation for Ecological Association inference (SPIEC-EASI) was applied to protist, invertebrate, and vertebrate compositional datasets to assess ASV-ASV co-occurrence patterns with depth across these datasets (Kurtz et al., 2015; Tipton et al., 2018). SPIEC-EASI identifies statistically significant relationships while accounting for issues inherent to compositional metabarcoding datasets (Kurtz et al., 2015). ASV count tables are CLR-transformed and a graphical model inference framework is used to identify direct associations between ASVs while minimizing indirect correlations and reducing the detection of spurious relationships.

Samples were grouped into three depth zones: epipelagic (10 m and 100 m), upper mesopelagic (300 m and 500 m), and lower mesopelagic (800 m and 1000 m). Out of a possible total of 24 samples in each depth zone, only samples that contained protist, invertebrate, and vertebrate ASVs were retained for network analysis, resulting in a total of 15 epipelagic samples, 21 upper mesopelagic samples, and 22 lower mesopelagic samples. ASVs were filtered on

abundance (> 50 reads) and prevalence (present in at least 10% of samples in each depth zone) to minimize dense networks and focus the analyses on prevalent and abundant ASVs.

Undirected networks were generated for each depth zone for metazoan-only (invertebrate and vertebrate) ASVs, protist-only ASVs, and all ASVs (All Taxa) for a total of nine networks. The SpiecEasi v1.1.1 package was used to construct these networks on WHOI's high-performance computing cluster in R v4.4.3, applying the Meinshausen–Buhlmann's neighborhood selection method with an optimal sparsity threshold (lambda min ratio) of 1e-3, and 100 subsampling replicates (rep.num = 100) (Kurtz et al., 2015).

In each network, edges (links) were inferred using SPIEC-EASI and represent signed conditional associations between ASVs (nodes) after accounting for indirect associations mediated by other ASVs. Positive edges indicate ASVs that exhibit similar relative abundance patterns across samples (co-vary in the same direction), whereas negative edges indicate ASVs that co-vary in opposite directions

Networks were then exported into RStudio to assess network topology and robustness with igraph v2.0.2 in R (Csárdi and Nepusz, 2006). For each network, we evaluated node and edge connectivity, which represents the minimum threshold for node or edge removal that fragments a connected network. We also evaluated attack robustness, which measures the size of the network (remaining subnetwork) as nodes are sequentially removed based on betweenness, degree, and at random (Iyer et al., 2013; Tipton et al., 2018).

Although ecological networks can be built from species-level or other taxonomic groups, we built networks from ASVs, the lowest genetic unit, to render an appropriate comparison across the three datasets generated from two markers of varying taxonomic resolution. For example, while 18S V9 is highly conserved and is useful for broad amplification of eukaryotic biodiversity, it has less resolving power than other markers like 12S MiFish, which can resolve to species level for a wide variety of fishes (Creer et al., 2016; Zhang et al., 2018; Miya et al., 2020; Govindarajan et al., 2021; Questel et al., 2021). To show this, we evaluated the three naïve Bayes classifiers

310 referenced in this study with the evaluate-fit-classifier function in the QIIME 2 RESCRIPt plugin
311 (Robeson et al., 2021) to test the classifiers' performance on the same sequences it was trained
312 with. The F-measure score, which reflects the balance between precision and recall, for the 18S
313 V9 classifiers drops below ~0.95 after Order while the 12S classifier has a high F-measure up to
314 species-level classification (Supplementary Figure S5). After networks were generated, ASVs
315 were grouped into relevant taxonomic groups of ecological and functional significance for
316 downstream network analyses.
317
318 **3.6 Visualizations**
319 Unless otherwise specified, figures were generated with ggplot2 v3.5.1 (Wickham, 2016).
320 UpSet plots were generated with ComplexUpset v1.3.3. Networks were visualized with ggnetwork
321 v0.5.13 (Tyner et al., 2017). When necessary, visualizations were compiled with minimal editing
322 for aesthetics with the creative software, Affinity Designer 2 (Serif, Europe).
323
324 **4. RESULTS**
325 **4.1 Patterns of diversity from 18S and 12S metabarcoding**
326 Metabarcoding of the 18S V9 rRNA gene generated ASVs for protists and invertebrates
327 while the 12S MiFish metabarcoding generated ASVs for vertebrates (predominately fishes). The
328 18S dataset ranged from 70-90% protist sequences with the proportion of invertebrate sequences
329 decreasing with depth (Supplementary Figure S6). Protist and invertebrate sequences were
330 parsed from the 18S dataset and assessed separately. Following decontamination and rarefaction
331 of metabarcoding reads, a total of 8112 ASVs were recovered across both markers with 7046
332 (86.9%) for protists, 399 (4.9%) for invertebrates, and 667 (8.2%) for vertebrates. The numbers
333 of observed ASVs (or ASV richness) for protists and invertebrates were generally higher in the
334 mesopelagic than the epipelagic with relatively constant richness across mesopelagic depths
335 (Figure 2). For vertebrates, higher richness was observed at 10 m and 500 m than at other depths.

For invertebrates, Shannon diversity indices were significantly different between surface (10 m) and all other depths ($p < 0.01$) while Pielou's evenness indices varied significantly at depth, especially between 100 m and select mesopelagic depths ($p < 0.05$). For vertebrates, average Shannon and Pielou's indices followed similar patterns as observed for ASV richness, although no significant differences were observed between depths (Supplementary Tables S5-S7). For protists however, Shannon and Pielou indices exhibited patterns that contrasted with those for richness. The highest Shannon diversity and Pielou evenness indices occurred at 100 m and then decreased with depth down to 500 m before increasing again to 1000 m.

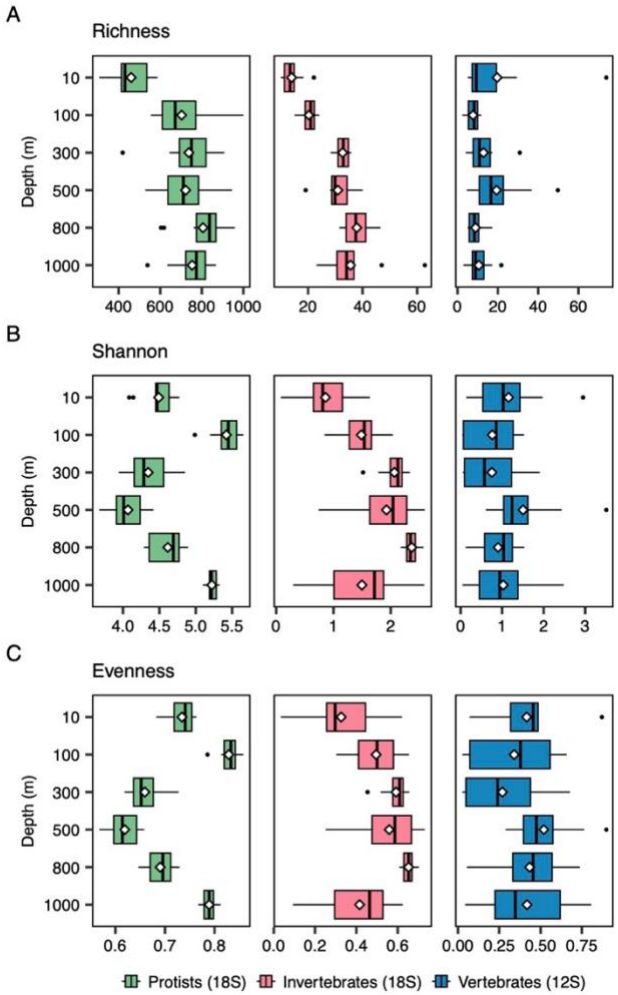

Figure 2. Patterns of alpha diversity with depth for A) Richness (observed ASVs), B) Shannon Diversity Index, and C) Pielou's Evenness Index across all samples for protists (n=69), invertebrates (n=70), and vertebrates (n=61). Boxplots show the variation in diversity indices at each depth between samples divided into quartiles with outlier values indicated by black points. A white diamond indicates the mean value at each depth.

379 Protistan diversity in epipelagic waters was comprised of mostly alveolates
380 (dinoflagellates, Syndiniales, and ciliates) and stramenopiles (e.g., diatoms) (Supplementary
381 Figure S7A). Alveolate ASVs increased in mesopelagic waters, as did rhizarian (e.g., radiolarians)
382 and excavate ASVs, with these three groups representing a significant portion of protistan
383 diversity (Supplementary Figure S7D). Invertebrate diversity was driven mainly by taxonomic
384 groups with relative read abundance < 1% (rare reads), including Trachymedusae and
385 Narcomedusae (Cnidaria) (Supplementary Figure S7B, Supplementary Table S3). Orders
386 Calanoida (calanoid copepods) and Siphonophorae (Cnidaria; siphonophores), as well as
387 unassigned metazoan ASVs, also represented a significant portion of diversity (Supplementary
388 Figure S7E). Fish were the main category of vertebrate ASVs detected (Supplementary Figure
389 S7C), with a significant portion attributed to deep sea fish taxa including Melamphidae (bigscales),
390 Myctophidae (lanternfish), and Gonostomatidae (bristlemouths). Similar to the invertebrates, rare
391 taxonomic groups (low read count) contributed significantly to vertebrate diversity (Supplementary
392 Figure S7F). Five mammalian ASVs were also detected, comprising ~0.038% of the total dataset.
393 These included ASVs assigned to whales and dolphins known to occur at the study site, including
394 two ASVs from the genus *Balaenoptera* (whales) and three ASVs for dolphins in the genera
395 *Delphinus*, *Stenella*, and *Grampus* (Supplementary Table S4).
396
397 **4.2 Depth structuring of the eukaryotic community**
398 Principal component analysis (PCA) and PERMANOVA of rarefied, center-log ratio (CLR)
399 transformed protist and invertebrate reads from all samples revealed significant depth clustering
400 ($p < 0.001$) (Figure 3). Moreover, pairwise comparison showed that communities at each depth
401 were significantly different from other depths ($p < 0.001$). For vertebrate communities, significant
402 differences were observed between surface (10 m) and mesopelagic depths ($p < 0.01$).
403 Differences were also found between 500 m and all other depths ($p < 0.05$). When all depths are
404 considered, clustering by CTD cast, which reflected the time of sampling, was not statistically

significant ($p > 0.05$). Given the limited number of CTD casts (two night and one day) and the lack of significant diel patterns in this dataset, samples across all three casts were combined at each depth for subsequent analyses (Supplementary Figures S8-S9, Supplementary Discussion).

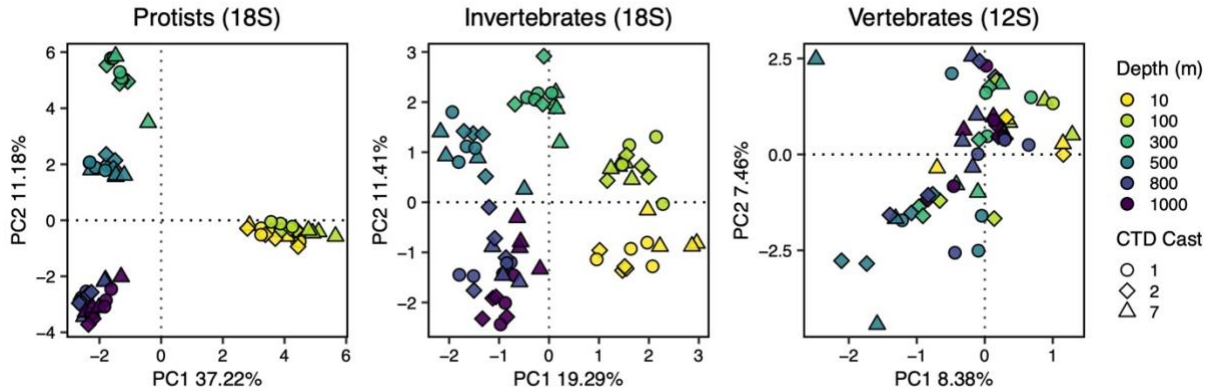

Figure 3. Principal component analysis (PCA) of center-log ratio-transformed reads for protists (n=69), invertebrates (n=70), and vertebrates (n=60). Each point represents one sample. The shape and color of each point indicates the CTD cast and the sampling depth, respectively, of each sample. CTD cast here can also reflect diel sampling with casts 1 and 7 sampled at midnight and cast 2 sampled during mid-day. One outlier (10 m, PC1 = ~10) from the vertebrate dataset was removed for visualization purposes (see Supplementary Figure S10).

Sequenced reads were aggregated by depth to generate relative abundance profiles that reflect the overall water column community structure (Figure 4). For protists, epipelagic (< 200 m) community structure was dominated by photosynthetic taxa including dinoflagellates, diatoms and other stramenopiles, and chlorophytes. The relative abundance of the parasitic taxon Syndiniales, as well as radiolarians, increased with depth and were the dominant taxa in the mesopelagic (> 200 m). Excavates were also relatively more abundant in deeper waters. For invertebrates, calanoid copepods (Arthropoda) exhibited higher relative abundance in both the epipelagic and lower mesopelagic (1000 m), while siphonophores (Cnidaria) were also relatively abundant, especially in the upper mesopelagic. At surface depths, salps were relatively abundant compared to other invertebrate taxa.

Key taxonomic groups were comprised of ASVs that were only detected at one specific depth (unique ASVs), detected at two or more depths (shared ASVs), or detected at all depths (cosmopolitan ASVs) (Supplementary Figure S11). Unique, shared, and cosmopolitan protist

ASVs included a mix of both photosynthetic and non-photosynthetic taxa across all depths with deeper waters harboring a higher number of unique ASVs than near the surface (10 m). Unique invertebrate ASVs were greater at mesopelagic depths and dominated by taxa with low relative abundance (< 1%), while unique vertebrate ASVs were highest at 10 m and 500 m. Across the three organismal groups, unique ASVs were proportionally higher than shared and cosmopolitan ASVs, especially for invertebrates (68.4%) and vertebrates (89.2%) compared to protists (56.6%).

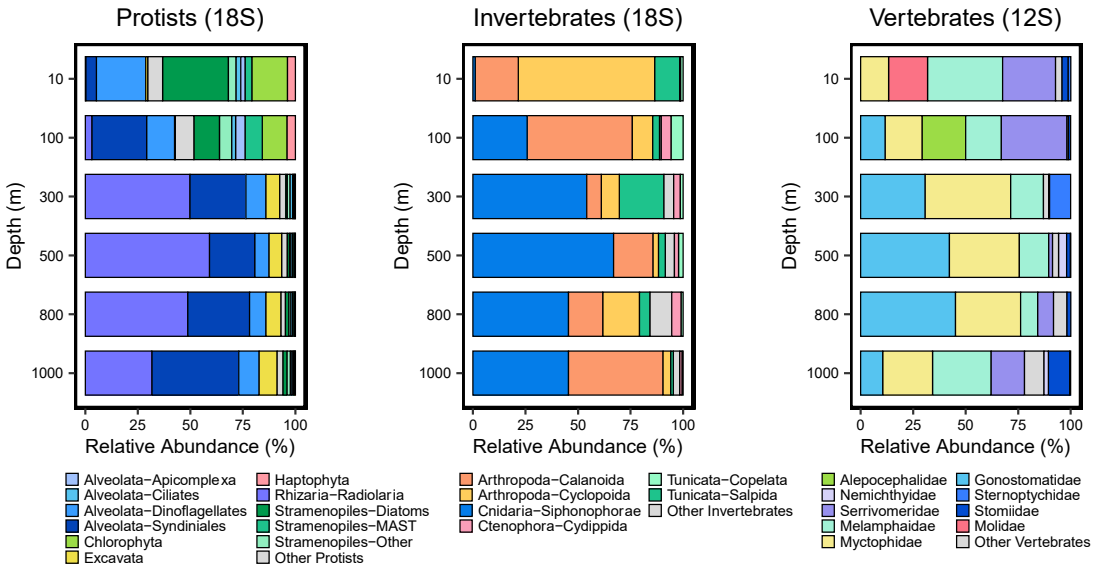

Figure 4. Depth profiles of relative read abundance (%) for protists, invertebrates, and vertebrates calculated from samples aggregated across three CTD casts. Bar plots show taxonomic groups in the order of decreasing relative abundance. In the legend, taxonomic groups within protists (Supergroup and/or Division or Subdivision) and invertebrates (Phylum and Order) are colored and listed in alphabetical order. Vertebrate families were grouped at the Order level in alphabetical order: Alepocephalidae (Alepocephaliformes); Nemichthyidae, Serrivomeridae (Anguilliformes); Melamphidae (Beryciformes); Myctophidae (Myctophiformes); Gonostomatidae, Sternoptychidae, Stomiidae (Stomiiformes); and Molidae (Tetraodontiformes). For each group, only taxa with overall relative abundance > 1% are displayed, with all other taxa combined in "Other". For a full list of "Other" taxa, see Supplementary Tables S2-S4.

For invertebrates, shared and cosmopolitan ASVs included representatives from Orders Calanoida (Arthropoda), Siphonophorae (Cnidaria), Cydippida (Ctenophora), as well as Copelata and Salpida (Tunicata) (Supplementary Figure S12). For vertebrates (Supplementary Figure S13), shared and cosmopolitan ASVs were observed from mesopelagic fish species including

Benthosema glaciale (Myctophidae), *Cyclothone microdon*, (Gonostomatidae), *Scopeloberyx opisthopterus* (Melamphaidae), and *Serrivomer beanii* (Serrivomeridae).

4.3 Depth-specific eukaryotic networks

We generated single-taxon and multi-trophic networks of protists, invertebrates, and vertebrates for the epipelagic (10 m and 100 m), upper mesopelagic (300 m and 500 m), and lower mesopelagic (800 m and 1000 m). Associations between “Metazoa-only” (invertebrates and vertebrates), “Protists-only”, and All Taxa (all groups) for each depth zone were inferred with SPIEC-EASI to assess the contribution of broad eukaryotic groups to network connectivity and stability.

Metazoa-only networks were small and fragmented, consisting of multiple components including singleton and doubleton associations that resulted in lower complexity networks compared to Protist-only and All Taxa networks (Figure 5, Supplementary Table S8). In contrast, Protist-only networks and All Taxa networks were fully connected such that a link existed between any two nodes in the network. Across all networks, the epipelagic had lower complexity (fewer nodes and edges) and decreased edge density (edge-to-node ratio) compared to the mesopelagic depths.

For each network, we assessed resilience and stability to the loss of ASVs. Node and edge connectivity increased with depth for All Taxa networks (Supplementary Table S8). The lower mesopelagic had the highest threshold for node and edge connectivity for both All Taxa and Protist networks. For the already fragmented Metazoa-only networks, connectivity was zero across all depth zones. We also evaluated attack robustness by which measuring the size of the remaining subnetwork as nodes are sequentially removed based on betweenness (putative bottlenecks or keystone taxa), degree (highly connected ASVs or hubs), and at random (Iyer et al., 2013; Tipton et al., 2018). Metazoa-only networks were the least robust, especially in the

476 mesopelagic. Protists-only and All Taxa networks had comparable robustness with higher
477 robustness in mesopelagic networks (Supplementary Figure S14).

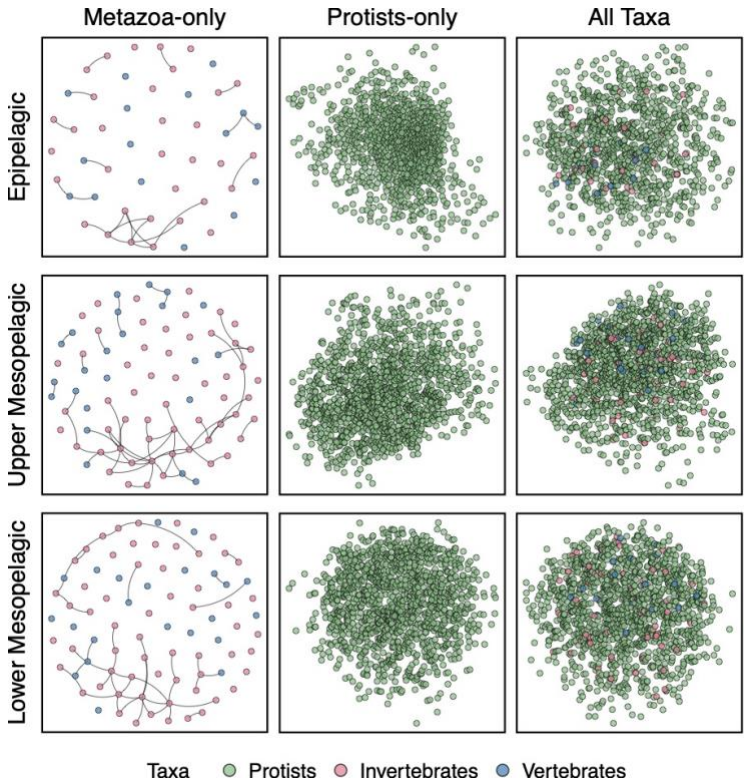

478

479 **Figure 5**. Depth-specific networks for Metazoa-only (invertebrate and vertebrates), Protists-only,
480 and All Taxa (all ASVs). All nodes are shown as points with color indicating the broad taxonomic
481 classification of protists, invertebrates, and vertebrates. Edges are shown for the Metazoa-only
482 network to show the fragmented nature of the network with singleton nodes. The Protists-only
483 and All Taxa networks are connected networks and edges are not shown. All networks include
484 predicted positive and negative interactions. A larger version of this figure is available as
485 Supplementary Figure S15.
486

487 **4.4 Ecological interactions from the surface to the mesopelagic**

488 Positive and negative interactions were separated from the combined networks to explore
489 putative ecological interactions, especially trophic dynamics across depth. While these networks
490 do not represent direct ecological interactions, associations between ASVs can be used to
491 hypothesize potential ecological relationships among taxa (Landi et al., 2018). Epipelagic and
492 upper mesopelagic networks averaged 58 and 57% positive interactions, respectively, while the
493 lower mesopelagic network was 53% positive (Supplementary Table S9). On average, the edge

density of positive networks was 8.1 compared to 6.5 for negative networks, suggesting that positive networks are more complex. Nodes were compartmentalized into modules that delineated subsets of ASVs that interact more frequently or have stronger interactions than with other ASVs (modularity). Average modularity across the three depth zones was higher for positive networks compared to negative networks (Supplementary Table S10). For both positive and negative networks, modularity decreased with depth. Node and edge connectivity for negative networks averaged 1.33 compared to an average of 2.67 for positive networks. Negative networks were also less robust than positive networks, especially in the epipelagic networks (Supplementary Figure S16).

Nodes with the highest edge weights (90th percentile), indicating the strongest interactions, were isolated from the positive and negative networks to explore key ASV associations in each network (Supplementary Figure S17). In both positive and negative subnetworks, the top ranking ASVs based on node degree (number of connections) and betweenness centrality were predominantly protistan taxa, especially Syndiniales (Alveolata) (Supplementary Figures S18-S19). Top ranking invertebrate ASVs included copepods (both calanoid and cyclopoid), siphonophores (cnidarians), and ctenophores while vertebrate ASVs included mesopelagic fish. Notably, *Grampus griseus* (Risso's dolphin) was a top-ranking ASV in the positive network, while salps (tunicates) and *Coryphaena hippurus* (common dolphinfish) were high-ranking ASVs in the negative network.

Trophic interactions were assessed by assuming a simple food web from the negative network where protists are at the bottom, invertebrates are intermediate, and vertebrates are top predators. In general, the total number of pair-wise associations (protist-invertebrate, protist-vertebrate, and invertebrate-vertebrate) were highest in the mesopelagic, with 1193 and 1088 associations in the upper and lower mesopelagic, respectively, compared to 582 associations in the epipelagic (Figure 6). We narrowed focus to the strongest interactions at each depth zone by selecting ASV-ASV associations with the top 10% of edge weights. Many of these strongest

relationships featured protist associations with both invertebrates and vertebrates and highlighted known interactions such as zooplankton grazing of phytoplankton, predator-prey dynamics between zooplankton and mesopelagic fish, as well as putative parasitic interactions between alveolates and various metazoans (Figure 6).

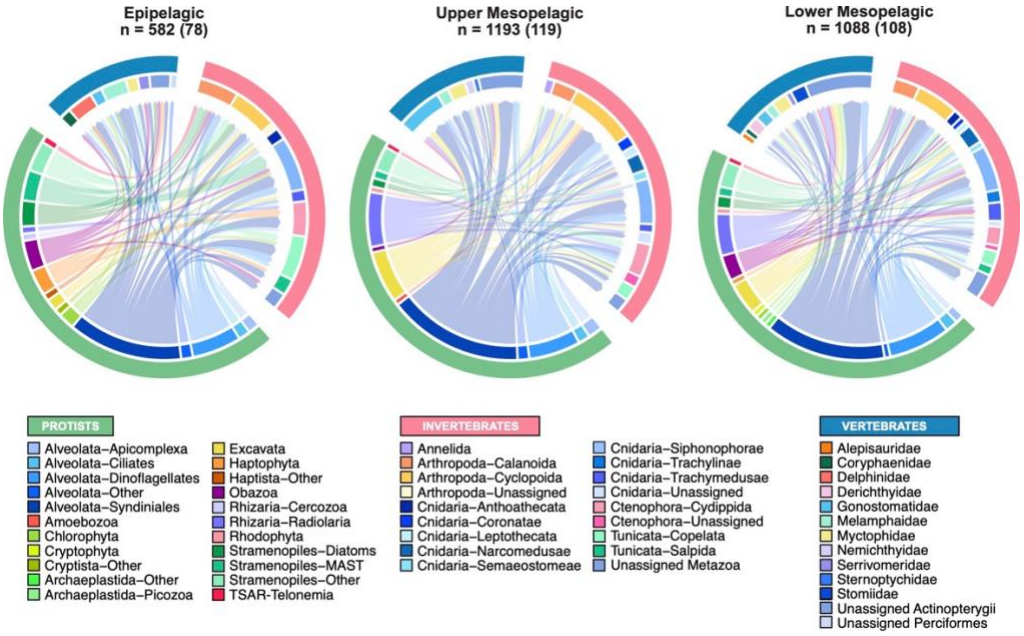

Figure 6. Chord diagrams indicate the number of strong pairwise interactions in the negative network and the taxonomic groups involved at each depth zone. Interactions were selected by removing all ASV-ASV linkages below the 90th percentile threshold for edge weight (so that only the strongest interactions remained). Only protist-invertebrate, protist-vertebrate, and invertebrate-vertebrate interactions were considered. The total number of pairwise associations for each negative network is listed (n) with the number of strong associations in parentheses. Colors along the circumference (track) of the diagram indicate taxonomic groupings. The outer track shows protists in green, invertebrates in pink, and vertebrates in blue. The inner track further divides these groupings into taxonomic groups. Each link between two ASVs (or interaction) is depicted as a directional arrow that starts from the ASV in a lower trophic level and points towards the ASV at the higher trophic level. The arrows are also colored based on the lower trophic level ASV. Trophic levels are simplified and ordered as protist > invertebrate > vertebrate. The size of each inner track segment indicates the relative number of ASVs under each taxonomic group within a chord diagram. A larger version of this figure is available as Supplementary Figures S20-S22.

5. DISCUSSION

5.1 Protists and metazoans exhibit contrasting diversity patterns

544 Based on current knowledge of the deep sea, we lack consensus on broad diversity trends
545 due to prevailing gaps across spatial, temporal, and taxonomic scales (Haddock and Choy, 2024;
546 Yang et al., 2024). Traditional midwater assessments often rely on net-based trawls, which
547 sample few depths and regions and can underrepresent taxa that avoid capture or are too fragile
548 (Kaartvedt et al., 2012; Gold et al., 2021; Suarez-Bregua et al., 2022). As such, deep sea studies
549 that span the eukaryotic community from microeukaryotes to metazoans remain scarce. Since we
550 applied multi-marker metabarcoding to eDNA, this study has generated new insights into
551 eukaryotic biodiversity and ecology from the surface down to the base of the mesopelagic.

552 A key finding of our study is that alpha diversity increased in the mesopelagic compared
553 to the epipelagic. We found this for both ASV diversity (richness) and Shannon diversity in the
554 Northwest Atlantic Slope Water, especially for protists and invertebrates. This observation differs
555 from the existing perspective of decreasing diversity in midwater ecosystems compared to
556 epipelagic waters generated from the global Ocean Biodiversity Information System (OBIS)
557 database (Costello and Chaudhary, 2017). However, Costello and Chaudhary did note a diversity
558 maximum at ~400-500 m, which aligns with our findings, especially for vertebrates (Figure 2). A
559 recent survey of more than two decades of ROV-generated data revealed taxa-specific patterns
560 in the eastern North Pacific such as higher species richness for crustaceans and fishes in the
561 mesopelagic compared to the epipelagic (Haddock and Choy, 2024).

562 While our findings generally show increasing alpha diversity with depth (Figure 2), we
563 observed low indices for protists between 300 m and 800 m with a minimum at 500 m. We
564 attributed the lower diversity in this depth zone to a small number of ASVs associated with
565 Syndiniales (Dinoflagellata) and Radiolaria (Rhizaria) that are highly abundant relative to other
566 ASVs (Supplementary Figure S23). Through the upper mesopelagic, this trend is generally in line
567 with previous studies that reported a protist diversity maximum at the base of the euphotic zone
568 followed by decreasing diversity in the mesopelagic (Laroche et al., 2020b; Blanco-Bercial et al.,

2022). In contrast, other studies have found increasing diversity in the mesopelagic, which we also observed in our dataset at 1000 m (Giner et al., 2020; Ollison et al., 2021).

We also found higher richness in the mesopelagic for invertebrates, which is similar to diversity metrics reported for other areas of the North Pacific (Matthews and Blanco-Bercial, 2023) as well as the southeast Pacific (González et al., 2023), but contrasting with diversity patterns reported off Hawaii (Laroche et al., 2020b). These studies showed that arthropods (especially copepods) and cnidarians are significant contributors to metazoan diversity. In addition, we found vertebrate diversity assessed with the 12S biomarker detected mainly fish. As with previous studies (Canals et al., 2021; Govindarajan et al., 2023b), a significant portion of sequencing reads were associated with deep-sea fish (Supplementary Figure S7).

For invertebrates and vertebrates, Shannon diversity was high across mesopelagic depths with the highest ASV richness at 500 m for vertebrates, which corresponded with the deep scattering layer detected at 38 kHz (Supplementary Figure S1), a region of the midwater with strong acoustic backscatter from mesopelagic fish and invertebrates (Barham, 1966; Aksnes et al., 2017). Taxonomic groups with low relative abundance (< 1%) or “rare” taxa typically contributed to alpha diversity for protists, invertebrates, and vertebrates (Supplementary Figure S7 and S11). While our study was not explicitly focused on the role of these low abundance taxa, these rare taxa may exert considerable influence over ecosystem function and stability (Lyons et al., 2005; Mouillot et al., 2013; Logares et al., 2014; Lynch and Neufeld, 2015; Jousset et al., 2017).

There are various factors that may contribute to the differences reported across metabarcoding studies. There are differences in methodology (e.g., primer selection, volume filtered, filter pore size or size fractionation, and number of samples), as well as study site (e.g., Atlantic or Pacific) and seasonal timing of sampling linked to varied environmental conditions that shape the community (Govindarajan et al., 2023a). For example, our study was conducted in the productive Northwest Atlantic Slope Water region and consisted of bulk water sampling (no size

fractionation) in March 2020, while the Blanco-Bercial et al. study (2022) was conducted monthly over the course of one year and the Giner et al. study (2020) used size-fractionated water samples (0.2-3 μm). Additionally, in our study, ASV accumulation curves for protists, invertebrates, and vertebrates suggested that the sampling scheme did not completely resolve the total biodiversity, which may also contribute to observed differences in diversity across studies.

Moreover, the chance encounter of a salp bloom during our sampling (see Methods) contributed to high relative abundance of salp sequences in surface waters (214) compared to other studies (Govindarajan et al., 2022; González et al., 2023; Matthews and Blanco-Bercial, 2023). Although we were unable to sample outside of the bloom to assess their impact on community composition, it is possible that diversity trends we observed may have been influenced by high salp densities. For example, previous studies suggest that salp blooms may impact biodiversity by substantially reducing phytoplankton biomass (Zeldis et al., 1995; Décima et al., 2023) and outcompeting other planktonic organisms for food (Paffenhöfer et al., 1995; Perissinotto and A. Pakhomov, 1998; Stukel et al., 2021).

Going forward, the maturation of multi-marker metabarcoding for deep sea studies will benefit from improved reference libraries for taxonomic assignments, increased spatial and temporal sampling, and standardization of sampling technologies, wet lab processes, and bioinformatics pipelines (McClenaghan et al., 2020; Patin and Goodwin, 2022; Kelly et al., 2023).

5.2 Eukaryotic community structure is depth-dependent

Eukaryotic communities were depth-dependent with differing community composition for protists, invertebrates, and vertebrates (Figure 3). Protist community composition was highly influenced by depth with distinct communities at each of our sampled depths and a notable shift in dominant taxa between epipelagic and mesopelagic depth zones. Invertebrate communities were also depth-specific, although there was more overlap across the communities with samples clustering into three depth bands for the epipelagic (< 200 m), upper mesopelagic (300-500 m),

621 and lower mesopelagic (> 500 m). Vertebrate communities were less structured with depth with
622 samples at 500 m exhibiting a significant difference between epipelagic and lower mesopelagic
623 samples. The diminished depth clustering coincides with greater organismal mobility from single-
624 celled protists to vertebrates, which may reflect a reduced depth constraint as swimming capacity
625 increases.

626 Depth-dependency of eukaryotic communities, especially for protists, has been
627 established previously, with a distinct transition in community composition between the sunlit
628 surface and the deep (Ollison et al., 2021; Blanco-Bercial et al., 2022; Yeh and Fuhrman, 2022;
629 Sun et al., 2023; Anderson et al., 2024). For protists, a high relative abundance of photosynthetic
630 taxa including stramenopiles and chlorophytes transitions into dominance by alveolates,
631 especially Syndiniales and radiolarians.

632 Similar to other metazoan studies, we found high relative abundance of calanoid copepods
633 (Order Calanoida) in the water column, as well as a subsurface abundance of Siphonophorae
634 and Ctenophora (e.g., comb jellies) (Laroche et al., 2020b; Govindarajan et al., 2021). For
635 vertebrates, we detected high relative abundance of mesopelagic fish from families Myctophidae
636 and Gonostomatidae, which were also present in other metabarcoding studies (Canals et al.,
637 2021; Govindarajan et al., 2023b; Dan et al., 2024). In epipelagic waters, additional taxa occurring
638 in high relative abundance included the families Serrivomeridae (sawtooth eels), Molidae (molas),
639 and Alepocephalidae (slickheads).

640 We did not detect strong signals of diel vertical migrators in our 18S and 12S datasets
641 (Figure 3). The 18S V9 biomarker used in this study amplifies many protistan and invertebrate
642 taxa, which can dilute the signal of migrating taxa. In a previous study with higher diel sampling
643 resolution, DVM was also not detected when using the 18S biomarker (Govindarajan et al., 2021).
644 For fishes, previous studies detected higher deep-sea species richness at night in surface waters
645 (Canals et al., 2021; Govindarajan et al., 2023b). However, we noted mainly lower species
646 richness at surface depths (Supplementary Table S11). The lack of strong DVM signals in our

647 datasets is likely due to a combination of factors including the sensitivity of eDNA approaches,
648 low diel sampling resolution with only three CTD casts, and the biomarker choice. Moreover, while
649 eDNA metabarcoding can capture a robust snapshot of the whole community biodiversity, it may
650 not accurately reflect the active community as eDNA in the water column originates from both
651 dead and living organisms and encompass whole cells and genetic material that is sloughed off
652 or excreted from moving animals (Allan et al., 2021b; Rodriguez-Ezpeleta et al., 2021). For
653 example, salps are known diel vertical migrators (Wiebe et al., 1979; Madin et al., 2006) and we
654 observed in situ DVM (Supplementary Figure S2). However, eDNA depth profiles were not as
655 clear with higher relative abundance in deeper waters during the night and day (Supplementary
656 Figure S24), which may be a result of eDNA sourced directly from salps or from sinking fecal
657 pellets (Govindarajan et al., 2021).

658 To probe potential signals of DVM, we instead focused our analyses on the presence of
659 unique, shared, and cosmopolitan ASVs across depth (Supplementary Figure S11). The detection
660 of unique ASVs could indicate niche specialization to different environmental conditions within a
661 given taxonomic group (Ollison et al., 2021; Anderson et al., 2024). Unexpectedly, we found
662 unique ASVs for diatoms and chlorophytes in deep waters. Rather than niche specialization of
663 these photosynthetic taxa to aphotic conditions, we hypothesize that these sequences indicate
664 export of primary producers out of the euphotic zone as sinking particles (Amacher et al., 2013;
665 Durkin et al., 2016, 2021, 2022; Mestre et al., 2018; Baumas and Bizic, 2024; Bodel et al., 2025;
666 Kramer et al., 2025).

667 Animals shed DNA as they move through the water column, and we hypothesize that
668 unique ASVs represent cohorts of animals that are non-migratory while shared and cosmopolitan
669 ASVs reflect migratory cohorts. However, another possible explanation for the high occurrence of
670 unique invertebrate and vertebrate ASVs may be due to under-sampling of metazoan biodiversity,
671 which tend to be patchily distributed in the water column. Accumulation curves for ASV richness
672 across our sample set suggest that additional sampling may be necessary to recover the true

673 community richness for metazoans, especially for fish (Supplementary Figure S25).
674 Environmental factors that influence eDNA shedding, persistence, and transport in combination
675 with low-volume (~1-5 L) sampling efforts impact eDNA recovery for metazoan detection
676 (Govindarajan et al., 2022, 2023a). While these volumes may be adequate for microbial studies,
677 they likely underestimate metazoan biodiversity in deep sea ecosystems (Govindarajan et al.,
678 2022), which can lead to a skewed perspective of their vertical and horizontal distribution.
679 However, unique and cosmopolitan ASVs can be used to probe DVM behaviors, which may be
680 useful to better understand the ecology of these otherwise elusive taxa that warrant further study.
681 We detected invertebrate and vertebrate ASVs that appeared at multiple sampling depths
682 (shared and cosmopolitan ASVs), which included representatives from known migratory
683 invertebrate taxa including copepods, cnidarians, and tunicates (Bianchi and Mislan, 2016;
684 Romero-Romero et al., 2019; Easson et al., 2020), as well as mesopelagic fish including
685 lanternfish and bristlemouths. Most of these fish are considered migratory except for *Cyclothone*
686 *microdon* (bristlemouth) and *Scopeloberyx opisthopterus* (bigscale), which are lower mesopelagic
687 and bathypelagic dwelling (Sutton, 2013; Govindarajan et al., 2023b; Richards et al., 2023).
688 However, our study detected one ASV each of *C. microdon* (15 ASVs total) and *S. opisthopterus*
689 (97 ASVs total) with a relatively high abundance in epipelagic waters, especially during the day.
690 While studies have indicated that juvenile stages of mesopelagic fish may occur at shallower
691 depths (Olivar and Beckley, 2022), it remains unclear whether the driving mechanism is
692 ontogenetic migration or other drivers such as niche expansion that require further study (Sutton
693 et al., 2008; Cook et al., 2013; Granata et al., 2023).
694
695 **5.3 Protists increase ecosystem complexity and stability**
696 Diversity (nodes or ASVs), connectivity (edges or interactions) and edge density (edge-
697 to-node ratio) are core determinants of network complexity (Landi et al., 2018; Espinoza et al.,
698 2020). Increasing biological diversity and their interactions increase ecosystem complexity, which

often correlates with enhanced stability or resilience (McCann, 2000; Dunne et al., 2002; Carpentier et al., 2021; Nauta and De Domenico, 2024). Our ecological network analyses from multi-marker metabarcoding of the eukaryotic community showed that protistan taxa play a key role in mediating trophic interactions and ecosystem function. While metazoan networks were fragmented, the addition of protistan ASVs increased diversity and interactions (Supplementary Table S7), producing fully connected networks at all depths with protist nodes facilitating interactions between previously unconnected metazoan nodes (Figure 5). Increased protistan diversity may stabilize connectivity by enhancing the likelihood that biological communities are resilient to environmental fluctuations and can compensate the loss of functionally important taxa (functional redundancy) (Naeem and Li, 1997; Naeem, 1998; McCann, 2000).

Alternatively, our fragmented ecological networks may reflect the more heterogenous distributions of metazoan taxa that reduce co-occurrences and interactions, especially in the vast and deep pelagic ocean where food is scarce (Robison, 2004; Ramirez-Llodra et al., 2010). Fragmented networks may also reflect sampling biases associated with low-volume samples, which may not provide a comprehensive snapshot of metazoan diversity and distribution compared to more easily sampled protistan taxa (Anderson and Thompson, 2022; Govindarajan et al., 2022). Significant knowledge gaps on metazoan eDNA further complicate our interpretation of metazoan eDNA signatures due in part to unknown rates of DNA shedding across different taxa and the varying impacts of environmental parameters on eDNA persistence (Allan et al., 2021a, 2021b; McCartin et al., 2022; Govindarajan et al., 2023a). Nevertheless, molecular tools like multi-marker metabarcoding and increasing availability of large-volume autonomous samplers are revolutionizing biodiversity research and provide important multi-trophic insights that are otherwise difficult to obtain, especially in the deep sea (Govindarajan et al., 2023a; Dan et al., 2024; Haddock and Choy, 2024; Yang et al., 2024).

5.4 Protists are key mediators of ecological interactions

725 Positive edges indicate ASVs that tend to exhibit similar co-variation patterns across
726 samples, whereas negative edges indicate opposing patterns. While signed associations do not
727 imply direct interactions, they provide a useful framework for generating hypotheses about
728 facilitative or antagonistic relationships that can be tested in future studies. Consistent with other
729 network studies, we interpret these associations as potentially reflecting shared or divergent
730 ecological responses. For example, positive interactions may indicate putative mutualistic or
731 commensal relationships while negative interactions suggest antagonistic relationships including
732 competition, predation, and parasitism (Xiao et al., 2017; Landi et al., 2018; Anderson et al., 2024;
733 Deutschmann et al., 2024). The balance of positive and negative interactions has been shown to
734 shape community interactions and ecosystem processes and in turn, ecological stability and
735 resilience to environmental change (Travis et al., 2005; Losapio et al., 2021). In our networks,
736 there were more positive interactions than negative interactions across all depth zones
737 (Supplementary Table S8), indicating an important role for mutualistic or facilitative relationships
738 in marine communities (Stachowicz, 2001; Deutschmann et al., 2024). The proportion of negative
739 interactions increased with depth, which may suggest that competition or predation dynamics
740 increases in importance in the relatively resource-scarce mesopelagic.

741 Positive networks were also more robust to node loss than negative networks and for both
742 network types, mesopelagic networks were more robust (Supplementary Figure S16). This may
743 be a result of the higher complexity found in the positive networks that can enhance network
744 stability. Moreover, positive networks had higher modularity, suggesting increased
745 compartmentalization of ASVs with potential niche partitioning and functional specialists
746 (Supplementary Table S8), which may also have a moderately stabilizing effect on networks. This
747 trend did not apply to depth-specific networks where positive and negative networks in the
748 epipelagic had higher modularity but lower robustness than mesopelagic networks. In our study,
749 decreased complexity in the epipelagic relative to mesopelagic depths is likely a stronger driver
750 of network stability. These dynamics suggest that negative-type interactions (e.g., key predator-

751 prey relationships), particularly in the epipelagic, may be more vulnerable to fragmentation or loss
752 of keystone taxa.

753 Top-ranking nodes indicating keystone taxa are highly connected ASVs that are important
754 facilitators of resource transfer (i.e., carbon and energy) throughout a network. A majority of the
755 top-ranking nodes in our study were protists (Supplementary Figures S18-S19), which included a
756 high number of ASVs belonging to the marine alveolate Syndiniales, suggesting an important role
757 for parasitism in the marine environment (Guillou et al., 2008; de Vargas et al., 2015; Anderson
758 et al., 2024). Copepod ASVs as well as various gelatinous taxa (cnidarians, ctenophores, and
759 salps), mesopelagic fish, and top predators (such as Risso's dolphin and common dolphinfish)
760 were also identified as keystone taxa (Supplementary Figures S18-19). Our findings highlight
761 protists as keystone taxa while also underscoring the importance of maintaining biodiversity
762 across trophic levels and functional groups to sustain ecosystem function and stability.

763 We identified known and previously unobserved trophic interactions in our simplified food
764 web analysis that featured protist associations with both invertebrates and vertebrates (Figure 6).
765 Protist-based associations were more common than invertebrate-vertebrate associations, which
766 were likely removed from consideration due to the low abundance and prevalence of metazoan
767 ASVs, especially for fish. Protist-driven associations likely play a key role in carbon export out of
768 the surface ocean and through deep sea food webs. For example, sinking particles and marine
769 snow harbor microbial communities comprised of senescent primary producers and diverse
770 microbial communities. Thus, our finding of protist-dominated interactions, especially in
771 mesopelagic networks, aligns with the consensus that marine snow is an important food source
772 in the deep sea (Dilling and Brzezinski, 2004; Choy et al., 2015; Cawley et al., 2021). Additionally,
773 these putative interactions likely do not reflect direct feeding relationships between protists and
774 metazoans, but may highlight indirect relationships between microorganisms and metazoans
775 linked by plankton-particle dynamics that contribute to overall ecosystem function and warrant
776 further study (Djurhuus et al., 2020; Holman et al., 2021; Doherty et al., 2025).

6. Conclusions

Mesopelagic studies that integrate both microorganisms and metazoans are rare, yet growing anthropogenic pressures underscore the need for more holistic research on this critical ocean realm. Our study applied a multi-marker metabarcoding approach to survey mesopelagic biodiversity in the Northwest Atlantic Slope Water region and construct ecological networks to examine mesopelagic diversity, organismal interactions, and ecosystem stability. Our findings revealed depth-specific structuring of the eukaryotic community, spanning protists, invertebrates, and vertebrates. We did not detect clear DVM patterns in our overall dataset, likely due to limited diel sampling. Assuming resource availability and feasibility, future sampling efforts should span across multiple day-night cycles to increase diel resolution. In addition, since eDNA originates from both living and dead organisms, incorporating environmental RNA as a more accurate approach for tracking DVM activity should be considered since RNA is only shed by living organisms (Cristescu, 2019; Yates et al., 2021).

Notably, ecological networks that included all eukaryotic groups were more robust than metazoan-only networks, with the incorporation of protist ASVs enhancing network complexity and stability. The higher diversity of protistan ASVs likely conferred resilience to taxa loss across mesopelagic networks compared to the epipelagic network. Additionally, we found that negative interactions were more vulnerable to taxa loss than positive interactions, with implications for carbon and energy transfer within food webs and deep-sea carbon sequestration. While mesopelagic networks appear more structurally stable, it is crucial to recognize that surface and deep-sea ecosystems are intrinsically linked through the biological carbon pump and vertically migrating organisms. Therefore, a more complete understanding of biodiversity, species interactions, and their impact on ecosystem function across spatial, temporal, and taxonomic scales is essential for effective ocean governance of the deep pelagic ocean.

Future work incorporating a cross-domain lens, inclusive of bacteria and archaea, and biogeochemical processes such as carbon flux (Guidi et al., 2016; Nguyen et al., 2022; McMonagle et al., 2024) will help us better understand the role of biodiversity and their interactions in facilitating carbon cycling and other critical ecosystem services.

7. Acknowledgments

We are grateful for everyone involved in the collection of environmental DNA samples including Rene Francolini and the crew of the R/V Armstrong. We also thank Erin Frates for laboratory processing of the samples. This research is part of the Woods Hole Oceanographic Institution's Ocean Twilight Zone Project, supported by funding as a part of The Audacious Project, a collaborative endeavor housed at TED and also funded in part by the National Oceanic and Atmospheric Administration's (NOAA's) Ocean Exploration Cooperative Institute under award NA19OAR4320072 to the University of Rhode Island (subaward number is 0007525/102212019 to WHOI).

8. References

Aitchson, J. (1986). *The statistical analysis of compositional data*., 1986th Edn. London, England: Chapman and Hall.

Aksnes, D. L., Røstad, A., Kaartvedt, S., Martinez, U., Duarte, C. M., and Irigoien, X. (2017). Light penetration structures the deep acoustic scattering layers in the global ocean. *Sci Adv* 3, e1602468.

Allan, E. A., DiBenedetto, M. H., Lavery, A. C., Govindarajan, A. F., and Zhang, W. G. (2021a). Modeling characterization of the vertical and temporal variability of environmental DNA in the mesopelagic ocean. *Sci. Rep.* 11, 21273.

Allan, E. A., Zhang, W. G., Lavery, A., and Govindarajan, A. (2021b). Environmental DNA shedding and decay rates from diverse animal forms and thermal regimes. *Environ. DNA* 3, 492–514.

Amacher, J., Neuer, S., and Lomas, M. (2013). DNA-based molecular fingerprinting of eukaryotic protists and cyanobacteria contributing to sinking particle flux at the Bermuda Atlantic time-series study. *Deep Sea Res. Part 2 Top. Stud. Oceanogr.* 93, 71–83.

Amaral-Zettler, L. A., McCliment, E. A., Ducklow, H. W., and Huse, S. M. (2009). A method for studying protistan diversity using massively parallel sequencing of V9 hypervariable regions of small-subunit ribosomal RNA genes. *PLoS One* 4, e6372.

Amon, D. J., Gollner, S., Morato, T., Smith, C. R., Chen, C., Christiansen, S., et al. (2022a). Assessment of scientific gaps related to the effective environmental management of deep-seabed mining. *Mar. Policy* 138, 105006.

Amon, D. J., Rotjan, R. D., Kennedy, B. R. C., Alleng, G., Anta, R., Aram, E., et al. (2022b). My Deep Sea, My Backyard: a pilot study to build capacity for global deep-ocean exploration and research. *Philos. Trans. R. Soc. Lond. B Biol. Sci.* 377, 20210121.

Anderson, S. R., Blanco-Bercial, L., Carlson, C. A., and Harvey, E. L. (2024). Role of Syndiniales parasites in depth-specific networks and carbon flux in the oligotrophic ocean. *ISME Commun* 4, ycae014.

Anderson, S. R., and Thompson, L. R. (2022). Optimizing an enclosed bead beating extraction method for microbial and fish environmental DNA. *Environ. DNA* 4, 291–303.

Arbizu, P. M. (2020). *pairwiseAdonis: Pairwise multilevel comparison using adonis. R package version 0.4*. Available at: https://github.com/pmartinezarbizu/pairwiseAdonis

Arístegui, J., Gasol, J. M., Duarte, C. M., and Herndld, G. J. (2009). Microbial oceanography of the dark ocean's pelagic realm. *Limnol. Oceanogr.* 54, 1501–1529.

Barham, E. G. (1966). Deep scattering layer migration and composition: observations from a diving saucer. *Science* 151, 1399–1403.

Bastiaanssen, T. F. S., Quinn, T. P., and Loughman, A. (2022). Bugs as features (part I): Concepts and foundations for the compositional data analysis of the microbiome-gut-brain axis. *arXiv [q-bio.GN]*. doi: 10.1038/s44220-023-00148-3

Baumas, C., and Bizic, M. (2024). A focus on different types of organic matter particles and their significance in the open ocean carbon cycle. *Prog. Oceanogr.* 224, 103233.

Bianchi, D., and Mislan, K. A. S. (2016). Global patterns of diel vertical migration times and velocities from acoustic data. *Limnol. Oceanogr.* 61, 353–364.

Bisson, K., McMonagle, H., Iglesias, I., Halfter, S., and Gallo, N. (2023). Five reasons to take the precautionary approach to deep sea exploitation. *Communications Earth & Environment* 4, 1–3.

Blancher, P., Lefrançois, E., Rimet, F., Vasselon, V., Argillier, C., Arle, J., et al. (2022). A strategy for successful integration of DNA-based methods in aquatic monitoring. *MBMG* 6, e85652.

Blanco-Bercial, L., Parsons, R., Bolaños, L. M., Johnson, R., Giovannoni, S. J., and Curry, R. (2022). The protist community traces seasonality and mesoscale hydrographic features in the oligotrophic Sargasso Sea. *Frontiers in Marine Science* 9. doi: 10.3389/fmars.2022.897140

Bodel, A., Estapa, M., and Durkin, C. A. (2025). Solitary phytoplankton cells sink in the mesopelagic ocean. *PLoS One* 20, e0321918.

Bolyen, E., Rideout, J. R., Dillon, M. R., Bokulich, N. A., Abnet, C. C., Al-Ghalith, G. A., et al. (2019). Reproducible, interactive, scalable and extensible microbiome data science using QIIME 2. *Nat. Biotechnol.* 37, 852–857.

Braun, C. D., Della Penna, A., Arostegui, M. C., Afonso, P., Berumen, M. L., Block, B. A., et al. (2023). Linking vertical movements of large pelagic predators with distribution patterns of biomass in the open ocean. *Proc. Natl. Acad. Sci. U. S. A.* 120, e2306357120.

Buesseler, K. O., Boyd, P. W., Black, E. E., and Siegel, D. A. (2020). Metrics that matter for assessing the ocean biological carbon pump. *Proc. Natl. Acad. Sci. U. S. A.* 117, 9679–9687.

Callahan, B. J., McMurdie, P. J., and Holmes, S. P. (2017). Exact sequence variants should replace operational taxonomic units in marker-gene data analysis. *ISME J.* 11, 2639–2643.

Callahan, B. J., McMurdie, P. J., Rosen, M. J., Han, A. W., Johnson, A. J. A., and Holmes, S. P. (2016). DADA2: High-resolution sample inference from Illumina amplicon data. *Nat. Methods* 13, 581–583.

Canals, O., Mendibil, I., Santos, M., Irigoien, X., and Rodríguez-Ezpeleta, N. (2021). Vertical stratification of environmental DNA in the open ocean captures ecological patterns and behavior of deep-sea fishes. *Limnology and Oceanography Letters* 6, 339–347.

Carpentier, C., Barabás, G., Spaak, J. W., and De Laender, F. (2021). Reinterpreting the relationship between number of species and number of links connects community structure and stability. *Nat Ecol Evol* 5, 1102–1109.

Cavan, E. L., Laurenceau-Cornec, E. C., Bressac, M., and Boyd, P. W. (2019). Exploring the ecology of the mesopelagic biological pump. *Prog. Oceanogr.* 176, 102125.

Cawley, G. F., Décima, M., Mast, A., and Prairie, J. C. (2021). The effect of phytoplankton properties on the ingestion of marine snow by Calanus pacificus. *J. Plankton Res.* 43, 957–973.

Chavez, F., Min, M., Pitz, K., Truelove, N., Baker, J., LaScala-Grunewald, D., et al. (2021). Observing life in the sea using environmental DNA. *Oceanography* 34, 102–119.

Choy, C. A., Popp, B. N., Hannides, C. C. S., and Drazen, J. C. (2015). Trophic structure and food resources of epipelagic and mesopelagic fishes in the North Pacific Subtropical Gyre ecosystem inferred from nitrogen isotopic compositions. *Limnol. Oceanogr.* 60, 1156–1171.

Coenen, A. R., Hu, S. K., Luo, E., Muratore, D., and Weitz, J. S. (2020). A Primer for Microbiome Time-Series Analysis. *Front. Genet.* 11, 310.

Cook, A. B., Sutton, T. T., Galbraith, J. K., and Vecchione, M. (2013). Deep-pelagic (0–3000m) fish assemblage structure over the Mid-Atlantic Ridge in the area of the Charlie-Gibbs Fracture Zone. *Deep Sea Res. Part 2 Top. Stud. Oceanogr.* 98, 279–291.

Costello, M. J., and Chaudhary, C. (2017). Marine Biodiversity, Biogeography, Deep-Sea Gradients, and Conservation. *Curr. Biol.* 27, R511–R527.

Creer, S., Deiner, K., Frey, S., Porazinska, D., Taberlet, P., Thomas, W. K., et al. (2016). The ecologist's field guide to sequence-based identification of biodiversity. *Methods Ecol. Evol.* 7, 1008–1018.

Cristescu, M. E. (2019). Can Environmental RNA Revolutionize Biodiversity Science? *Trends Ecol. Evol.* 34, 694–697.

Csárdi, G., and Nepusz, T. (2006). The igraph software package for complex network research. Available at: https://www.semanticscholar.org/paper/1d2744b83519657f5f2610698a8ddd177ced4f5c (Accessed July 14, 2024).

Dan, M. E., Portner, E. J., Bowman, J. S., Semmens, B. X., Owens, S. M., Greenwald, S. M., et al. (2024). Using low volume eDNA methods to sample pelagic marine animal assemblages. *PLoS One* 19, e0303263.

Davis, N. M., Proctor, D. M., Holmes, S. P., Relman, D. A., and Callahan, B. J. (2018). Simple statistical identification and removal of contaminant sequences in marker-gene and metagenomics data. *Microbiome* 6, 226.

Davison, P. C., Checkley, D. M., Jr, Koslow, J. A., and Barlow, J. (2013). Carbon export mediated by mesopelagic fishes in the northeast Pacific Ocean. *Prog. Oceanogr.* 116, 14–30.

De Brauwer, M., Clarke, L. J., Chariton, A., Cooper, M. K., de Bruyn, M., Furlan, E., et al. (2023). Best practice guidelines for environmental DNA biomonitoring in Australia and New Zealand. *Environ. DNA* 5, 417–423.

de Vargas, C., Audic, S., Henry, N., Decelle, J., Mahé, F., Logares, R., et al. (2015). Ocean plankton. Eukaryotic plankton diversity in the sunlit ocean. *Science* 348, 1261605.

Décima, M., Stukel, M. R., Nodder, S. D., Gutiérrez-Rodríguez, A., Selph, K. E., Dos Santos, A. L., et al. (2023). Salp blooms drive strong increases in passive carbon export in the Southern Ocean. *Nat. Commun.* 14, 425.

Deiner, K., Bik, H. M., Mächler, E., Seymour, M., Lacoursière-Roussel, A., Altermatt, F., et al. (2017). Environmental DNA metabarcoding: Transforming how we survey animal and plant communities. *Mol. Ecol.* 26, 5872–5895.

Deutschmann, I. M., Delage, E., Giner, C. R., Sebastián, M., Poulain, J., Arístegui, J., et al. (2024). Disentangling microbial networks across pelagic zones in the tropical and subtropical global ocean. *Nat. Commun.* 15, 126.

Dilling, L., and Brzezinski, M. A. (2004). Quantifying marine snow as a food choice for zooplankton using stable silicon isotope tracers. *J. Plankton Res.* 26, 1105–1114.

Djurhuus, A., Closek, C. J., Kelly, R. P., Pitz, K. J., Michisaki, R. P., Starks, H. A., et al. (2020). Environmental DNA reveals seasonal shifts and potential interactions in a marine community. *Nat. Commun.* 11, 254.

Doherty, S. C., Choy, C. A., Paul, N. L., and Close, H. G. (2025). Microbial and metazoan activity in Monterey Bay, CA recorded in nitrogen isotope ratios of sinking and suspended particles. *J. Geophys. Res. Oceans* 130, e2025JC022372.

Dowd, M. H., Assad, V. E., Cazares-Nuesser, A. E., Drazen, J. C., Goetze, E., White, A. E., et al. (2025). Deep-sea mining discharge can disrupt midwater food webs. *Nat. Commun.* 16, 9575.

Drazen, J. C., Smith, C. R., Gjerde, K. M., Haddock, S. H. D., Carter, G. S., Choy, C. A., et al. (2020). Midwater ecosystems must be considered when evaluating environmental risks of deep-sea mining. *Proceedings of the National Academy of Sciences* 117, 17455–17460.

Dunne, J. A., Williams, R. J., and Martinez, N. D. (2002). Network structure and biodiversity loss in food webs: robustness increases with connectance. *Ecol. Lett.* 5, 558–567.

Durkin, C. A., Buesseler, K. O., Cetinić, I., Estapa, M. L., Kelly, R. P., and Omand, M. (2021). A Visual Tour of Carbon Export by Sinking Particles. *Global Biogeochem. Cycles* 35, e2021GB006985.

Durkin, C. A., Cetinić, I., Estapa, M., Ljubešić, Z., Mucko, M., Neeley, A., et al. (2022). Tracing the path of carbon export in the ocean though DNA sequencing of individual sinking particles. *ISME J.* 16, 1896–1906.

Durkin, C. A., Van Mooy, B. A. S., Dyhrman, S. T., and Buesseler, K. O. (2016). Sinking phytoplankton associated with carbon flux in the Atlantic Ocean: Sinking phytoplankton and carbon flux. *Limnol. Oceanogr.* 61, 1172–1187.

Easson, C. G., Boswell, K. M., Tucker, N., Warren, J. D., and Lopez, J. V. (2020). Combined eDNA and Acoustic Analysis Reflects Diel Vertical Migration of Mixed Consortia in the Gulf of Mexico. *Frontiers in Marine Science* 7. doi: 10.3389/fmars.2020.00552

Espinoza, J. L., Shah, N., Singh, S., Nelson, K. E., and Dupont, C. L. (2020). Applications of weighted association networks applied to compositional data in biology. *Environ. Microbiol.* 22, 3020–3038.

Giner, C. R., Pernice, M. C., Balagué, V., Duarte, C. M., Gasol, J. M., Logares, R., et al. (2020). Marked changes in diversity and relative activity of picoeukaryotes with depth in the world ocean. *ISME J.* 14, 437–449.

Gold, Z., Sprague, J., Kushner, D. J., Zerecero Marin, E., and Barber, P. H. (2021). eDNA metabarcoding as a biomonitoring tool for marine protected areas. *PLoS One* 16, e0238557.

Gold, Z., Wall, A. R., Schweizer, T. M., Pentcheff, N. D., Curd, E. E., Barber, P. H., et al. (2022). A manager's guide to using eDNA metabarcoding in marine ecosystems. *PeerJ* 10, e14071.

González, C. E., Blanco-Bercial, L., Escribano, R., Fernández-Urruzola, I., Rivera, R., and Ulloa, O. (2023). Revealing zooplankton diversity in the midnight zone. *Frontiers in Marine Science* 10. doi: 10.3389/fmars.2023.1252535

Govindarajan, A. F., Adams, A., Allan, E., Herrera, S., Lavery, A., Llopiz, J., et al. (2023a). Advances in environmental DNA sampling for observing ocean twilight zone animal diversity. *Oceanography*. doi: 10.5670/oceanog.2023.s1.27

Govindarajan, A. F., Francolini, R. D., Jech, J. M., Lavery, A. C., Llopiz, J. K., Wiebe, P. H., et al. (2021). Exploring the Use of Environmental DNA (eDNA) to Detect Animal Taxa in the Mesopelagic Zone. *Frontiers in Ecology and Evolution* 9. doi: 10.3389/fevo.2021.574877

Govindarajan, A. F., Llopiz, J. K., Caiger, P. E., Jech, J. M., Lavery, A. C., McMonagle, H., et al. (2023b). Assessing mesopelagic fish diversity and diel vertical migration with environmental DNA. *Frontiers in Marine Science* 10. doi: 10.3389/fmars.2023.1219993

Govindarajan, A. F., McCartin, L., Adams, A., Allan, E., Belani, A., Francolini, R., et al. (2022). Improved biodiversity detection using a large-volume environmental DNA sampler with in situ filtration and implications for marine eDNA sampling strategies. *Deep Sea Res. Part I* 189, 103871.

Granata, A., Bergamasco, A., Zagami, G., Guglielmo, R., Bonanzinga, V., Minutoli, R., et al. (2023). Daily vertical distribution and diet of Cyclothone braueri (Gonostomatidae) in the Polcevera submarine canyon (Ligurian Sea, north-western Mediterranean). *Deep Sea Res. Part I* 199, 104113.

Groeneveld, J., Berger, U., Henschke, N., Pakhomov, E. A., Reiss, C. S., and Meyer, B. (2020). Blooms of a key grazer in the Southern Ocean – An individual-based model of Salpa thompsoni. *Prog. Oceanogr.* 185, 102339.

Guidi, L., Chaffron, S., Bittner, L., Eveillard, D., Larhlimi, A., Roux, S., et al. (2016). Plankton networks driving carbon export in the oligotrophic ocean. *Nature* 532, 465–470.

Guillou, L., Bachar, D., Audic, S., Bass, D., Berney, C., Bittner, L., et al. (2013). The Protist Ribosomal Reference database (PR2): a catalog of unicellular eukaryote small sub-unit rRNA sequences with curated taxonomy. *Nucleic Acids Res.* 41, D597-604.

Guillou, L., Viprey, M., Chambouvet, A., Welsh, R. M., Kirkham, A. R., Massana, R., et al. (2008). Widespread occurrence and genetic diversity of marine parasitoids belonging to Syndiniales (Alveolata). *Environ. Microbiol.* 10, 3349–3365.

Haddock, S. H. D., and Choy, C. A. (2024). Life in the Midwater: The Ecology of Deep Pelagic Animals. *Ann. Rev. Mar. Sci.* 16, 383–416.

Hemsley, V., Füssel, J., Duret, M. T., Rayne, R. R., Iversen, M. H., Henson, S. A., et al. (2023). Suspended particles are hotspots of microbial remineralization in the ocean's twilight zone. *Deep Sea Res. Part 2 Top. Stud. Oceanogr.* 212, 105339.

Hernández-León, S. (2023). The biological carbon pump, diel vertical migration, and carbon dioxide removal. *iScience* 26, 107835.

Herndl, G. J., and Reinthaler, T. (2013). Microbial control of the dark end of the biological pump. *Nat. Geosci.* 6, 718–724.

Holman, L. E., de Bruyn, M., Creer, S., Carvalho, G., Robidart, J., and Rius, M. (2021). Animals, protists and bacteria share marine biogeographic patterns. *Nat Ecol Evol* 5, 738–746.

Iglesias, I. S., Santora, J. A., Fiechter, J., and Field, J. C. (2023). Mesopelagic fishes are important prey for a diversity of predators. *Frontiers in Marine Science* 10. doi: 10.3389/fmars.2023.1220088

Iyer, S., Killingback, T., Sundaram, B., and Wang, Z. (2013). Attack robustness and centrality of complex networks. *PLoS One* 8, e59613.

Jousset, A., Bienhold, C., Chatzinotas, A., Gallien, L., Gobet, A., Kurm, V., et al. (2017). Where less may be more: how the rare biosphere pulls ecosystems strings. *ISME J.* 11, 853–862.

Kaartvedt, S., Staby, A., and Aksnes, D. L. (2012). Efficient trawl avoidance by mesopelagic fishes causes large underestimation of their biomass. *Mar. Ecol. Prog. Ser.* 456, 1–6.

Kelly, R. P., Lodge, D. M., Lee, K. N., Theroux, S., Sepulveda, A. J., Scholin, C. A., et al. (2023). Toward a national eDNA strategy for the United States. *Environ. DNA*. doi: 10.1002/edn3.432

Kramer, S. J., Jones, E. L., Estapa, M. L., Paul, N. L., Rynearson, T. A., Santoro, A. E., et al. (2025). Sinking particles exporting diatoms and Hacrobia predict the magnitude of oceanic POC flux. *ISME J.* 19, wraf105.

Kurtz, Z. D., Müller, C. L., Miraldi, E. R., Littman, D. R., Blaser, M. J., and Bonneau, R. A. (2015). Sparse and compositionally robust inference of microbial ecological networks. *PLoS Comput. Biol.* 11, e1004226.

Landi, P., Minoarivelo, H. O., Brännström, Å., Hui, C., and Dieckmann, U. (2018). Complexity and stability of ecological networks: a review of the theory. *Popul. Ecol.* 60, 319–345.

Laroche, O., Kersten, O., Smith, C. R., and Goetze, E. (2020a). Environmental DNA surveys detect distinct metazoan communities across abyssal plains and seamounts in the western Clarion Clipperton Zone. *Mol. Ecol.* 29, 4588–4604.

Laroche, O., Kersten, O., Smith, C. R., and Goetze, E. (2020b). From Sea Surface to Seafloor: A Benthic Allochthonous eDNA Survey for the Abyssal Ocean. *Frontiers in Marine Science* 7. doi: 10.3389/fmars.2020.00682

Logares, R., Audic, S., Bass, D., Bittner, L., Boutte, C., Christen, R., et al. (2014). Patterns of rare and abundant marine microbial eukaryotes. *Curr. Biol.* 24, 813–821.

Losapio, G., Schöb, C., Staniczenko, P. P. A., Carrara, F., Palamara, G. M., De Moraes, C. M., et al. (2021). Network motifs involving both competition and facilitation predict biodiversity in alpine plant communities. *Proc. Natl. Acad. Sci. U. S. A.* 118. doi: 10.1073/pnas.2005759118

Lynch, M. D. J., and Neufeld, J. D. (2015). Ecology and exploration of the rare biosphere. *Nat. Rev. Microbiol.* 13, 217–229.

Lyons, K. G., Brigham, C. A., Traut, B. H., and Schwartz, M. W. (2005). Rare species and ecosystem functioning: Rare species and ecosystem functioning. *Conserv. Biol.* 19, 1019–1024.

Madin, L. P., Kremer, P., Wiebe, P. H., Purcell, J. E., Horgan, E. H., and Nemazie, D. A. (2006). Periodic swarms of the salp Salpa aspera in the Slope Water off the NE United States: Biovolume, vertical migration, grazing, and vertical flux. *Deep Sea Res. Part 1 Oceanogr. Res. Pap.* 53, 804–819.

Martin, A., Boyd, P., Buesseler, K., Cetinic, I., Claustre, H., Giering, S., et al. (2020). The oceans' twilight zone must be studied now, before it is too late. *Nature Publishing Group UK*. doi: 10.1038/d41586-020-00915-7

Martin, M. (2011). Cutadapt removes adapter sequences from high-throughput sequencing reads. *EMBnet J.* 17, 10.

Matthews, S. A., and Blanco-Bercial, L. (2023). Divergent patterns of zooplankton connectivity in the epipelagic and mesopelagic zones of the eastern North Pacific. *Ecol. Evol.* 13, e10664.

Mazuecos, I. P., Arístegui, J., Vázquez-Domínguez, E., Ortega-Retuerta, E., Gasol, J. M., and Reche, I. (2015). Temperature control of microbial respiration and growth efficiency in the

mesopelagic zone of the South Atlantic and Indian Oceans. *Deep Sea Res. Part I* 95, 131–138.

McCann, K. S. (2000). The diversity-stability debate. *Nature* 405, 228–233.

McCartin, L. J., Vohsen, S. A., Ambrose, S. W., Layden, M., McFadden, C. S., Cordes, E. E., et al. (2022). Temperature Controls eDNA Persistence across Physicochemical Conditions in Seawater. *Environ. Sci. Technol.* 56, 8629–8639.

McClenaghan, B., Fahner, N., Cote, D., Chawarski, J., McCarthy, A., Rajabi, H., et al. (2020). Harnessing the power of eDNA metabarcoding for the detection of deep-sea fishes. *PLoS One* 15, e0236540.

McMonagle, H., Llopiz, J. K., Maas, A. E., Steinberg, D. K., Govindarajan, A. F., and Essington, T. E. (2024). Quantifying uncertainty in the contribution of mesopelagic fishes to the biological carbon pump in the Northeast Atlantic Ocean. *ICES J. Mar. Sci.* 81, 2037–2051.

McMurdie, P. J., and Holmes, S. (2013). phyloseq: an R package for reproducible interactive analysis and graphics of microbiome census data. *PLoS One* 8, e61217.

Mestre, M., Ruiz-González, C., Logares, R., Duarte, C. M., Gasol, J. M., and Sala, M. M. (2018). Sinking particles promote vertical connectivity in the ocean microbiome. *Proc. Natl. Acad. Sci. U. S. A.* 115, E6799–E6807.

Miya, M., Gotoh, R. O., and Sado, T. (2020). MiFish metabarcoding: a high-throughput approach for simultaneous detection of multiple fish species from environmental DNA and other samples. *Fish. Sci.* 86, 939–970.

Miya, M., Sato, Y., Fukunaga, T., Sado, T., Poulsen, J. Y., Sato, K., et al. (2015). MiFish, a set of universal PCR primers for metabarcoding environmental DNA from fishes: detection of more than 230 subtropical marine species. *R Soc Open Sci* 2, 150088.

Mouillot, D., Bellwood, D. R., Baraloto, C., Chave, J., Galzin, R., Harmelin-Vivien, M., et al. (2013). Rare species support vulnerable functions in high-diversity ecosystems. *PLoS Biol.* 11, e1001569.

Naeem, S. (1998). Species redundancy and ecosystem reliability. *Conserv. Biol.* 12, 39–45.

Naeem, S., and Li, S. (1997). Biodiversity enhances ecosystem reliability. *Nature* 390, 507–509.

Nauta, J., and De Domenico, M. (2024). Topological conditions drive stability in meta-ecosystems. *Phys. Rev. Res.* 6, 043055.

Nguyen, T. T. H., Zakem, E. J., Ebrahimi, A., Schwartzman, J., Caglar, T., Amarnath, K., et al. (2022). Microbes contribute to setting the ocean carbon flux by altering the fate of sinking particulates. *Nat. Commun.* 13, 1657.

O'Brien, T. D., Blanco-Bercial, L., Questel, J. M., Batta-Lona, P. G., and Bucklin, A. (2024). "MetaZooGene Atlas and Database: Reference Sequences for Marine Ecosystems," in *DNA Barcoding: Methods and Protocols*, ed. R. DeSalle (New York, NY: Springer US), 475–489.

Oksanen, J., Simpson, G., Blanchet, F., Kindt, R., Legendre, P., Minchin, P., et al. (2022). vegan: Community Ecology Package. R package version 2.6-4. Available at: https://CRAN.R-project.org/package=vegan

Olivar, M. P., and Beckley, L. E. (2022). Vertical distribution patterns of early stages of mesopelagic fishes along 110 °E, south-east Indian Ocean. *Deep Sea Res. Part 2 Top. Stud. Oceanogr.* 201, 105111.

Oliver, T. H., Heard, M. S., Isaac, N. J. B., Roy, D. B., Procter, D., Eigenbrod, F., et al. (2015). Biodiversity and Resilience of Ecosystem Functions. *Trends Ecol. Evol.* 30, 673–684.

Ollison, G. A., Hu, S. K., Mesrop, L. Y., DeLong, E. F., and Caron, D. A. (2021). Come rain or shine: Depth not season shapes the active protistan community at station ALOHA in the North Pacific Subtropical Gyre. *Deep Sea Res. Part I* 170, 103494.

Oschlies, A., Bach, L. T., Fennel, K., Gattuso, J.-P., and Mengis, N. (2025). Perspectives and challenges of marine carbon dioxide removal. *Front. Clim.* 6, 1506181.

Paffenhöfer, G.-A., Atkinson, L. P., Lee, T. N., Verity, P. G., and Bulluck, L. R., III (1995). Distribution and abundance of thaliaceans and copepods off the southeastern U.S.A. during winter. *Cont. Shelf Res.* 15, 255–280.

Patin, N. V., and Goodwin, K. D. (2022). Capturing marine microbiomes and environmental DNA: A field sampling guide. *Front. Microbiol.* 13, 1026596.

Pedregosa, F., Varoquaux, G., Gramfort, A., Michel, V., Thirion, B., Grisel, O., et al. (2011). Scikit-learn: Machine Learning in Python. *J. Mach. Learn. Res.* abs/1201.0490, 2825–2830.

Perissinotto, R., and A. Pakhomov, E. (1998). The trophic role of the tunicate Salpa thompsoni in the Antarctic marine ecosystem. *J. Mar. Syst.* 17, 361–374.

Pitz, K., Truelove, N., Nye, C., Michisaki, R. P., and Chavez, F. (2020). Environmental DNA (eDNA) 12S Metabarcoding Illumina MiSeq NGS PCR Protocol (Touchdown). Available at: https://www.protocols.io/view/environmental-dna-edna-12s-metabarcoding-illumina-kqdg35kqzv25/v2?step=6 (Accessed October 24, 2023).

Pruesse, E., Quast, C., Knittel, K., Fuchs, B. M., Ludwig, W., Peplies, J., et al. (2007). SILVA: a comprehensive online resource for quality checked and aligned ribosomal RNA sequence data compatible with ARB. *Nucleic Acids Res.* 35, 7188–7196.

Quast, C., Pruesse, E., Yilmaz, P., Gerken, J., Schweer, T., Yarza, P., et al. (2013). The SILVA ribosomal RNA gene database project: improved data processing and web-based tools. *Nucleic Acids Res.* 41, D590-6.

Questel, J. M., Hopcroft, R. R., DeHart, H. M., Smoot, C. A., Kosobokova, K. N., and Bucklin, A. (2021). Metabarcoding of zooplankton diversity within the Chukchi Borderland, Arctic Ocean: improved resolution from multi-gene markers and region-specific DNA databases. *Mar. Biodivers.* 51, 4.

Quinn, T. P., Erb, I., Richardson, M. F., and Crowley, T. M. (2018). Understanding sequencing data as compositions: an outlook and review. *Bioinformatics* 34, 2870–2878.

Ramirez-Llodra, E., Brandt, A., Danovaro, R., De Mol, B., Escobar, E., German, C. R., et al. (2010). Deep, diverse and definitely different: unique attributes of the world's largest ecosystem. *Biogeosciences* 7, 2851–2899.

Richards, T. M., Sutton, T. T., Woodstock, M. S., Judkins, H., and David Wells, R. J. (2023). Body size, depth of occurrence, and local oceanography shape trophic structure in a diverse deep-pelagic micronekton assemblage. *Prog. Oceanogr.* 213, 102998.

Robeson, M. S., 2nd, O'Rourke, D. R., Kaehler, B. D., Ziemski, M., Dillon, M. R., Foster, J. T., et al. (2021). RESCRIPt: Reproducible sequence taxonomy reference database management. *PLoS Comput. Biol.* 17, e1009581.

Robinson, C., Steinberg, D. K., Anderson, T. R., Arístegui, J., Carlson, C. A., Frost, J. R., et al. (2010). Mesopelagic zone ecology and biogeochemistry – a synthesis. *Deep Sea Res. Part 2 Top. Stud. Oceanogr.* 57, 1504–1518.

Robison, B. H. (2004). Deep pelagic biology. *J. Exp. Mar. Bio. Ecol.* 300, 253–272.

Rodriguez-Ezpeleta, N., Morissette, O., Bean, C. W., Manu, S., Banerjee, P., Lacoursière-Roussel, A., et al. (2021). Trade-offs between reducing complex terminology and producing accurate interpretations from environmental DNA: Comment on "Environmental DNA: What's behind the term?" by Pawlowski et al., (2020). *Mol. Ecol.* 30, 4601–4605.

Romero-Romero, S., Choy, C. A., Hannides, C. C. S., Popp, B. N., and Drazen, J. C. (2019). Differences in the trophic ecology of micronekton driven by diel vertical migration. *Limnol. Oceanogr.* 64, 1473–1483.

Sala, E., Mayorga, J., Bradley, D., Cabral, R. B., Atwood, T. B., Auber, A., et al. (2021). Protecting the global ocean for biodiversity, food and climate. *Nature* 592, 397–402.

Schloss, P. D. (2024a). Rarefaction is currently the best approach to control for uneven sequencing effort in amplicon sequence analyses. *mSphere* 9, e0035423.

Schloss, P. D. (2024b). Waste not, want not: revisiting the analysis that called into question the practice of rarefaction. *mSphere* 9, e0035523.

St. John, M. A., Borja, A., Chust, G., Heath, M., Grigorov, I., Mariani, P., et al. (2016). A Dark Hole in Our Understanding of Marine Ecosystems and Their Services: Perspectives from the Mesopelagic Community. *Frontiers in Marine Science* 3. doi: 10.3389/fmars.2016.00031

Stachowicz, J. J. (2001). Mutualism, facilitation, and the structure of ecological communities. *Bioscience* 51, 235.

Stukel, M. R., Décima, M., Selph, K. E., and Gutiérrez-Rodríguez, A. (2021). Size-specific grazing and competitive interactions between large salps and protistan grazers. *Limnol. Oceanogr.* 66, 2521–2534.

Suarez-Bregua, P., Álvarez-González, M., Parsons, K. M., Rotllant, J., Pierce, G. J., and Saavedra, C. (2022). Environmental DNA (eDNA) for monitoring marine mammals: Challenges and opportunities. *Frontiers in Marine Science* 9. doi: 10.3389/fmars.2022.987774

Sun, P., Wang, Y., Zhang, Y., Logares, R., Cheng, P., Xu, D., et al. (2023). From the Sunlit to the Aphotic Zone: Assembly Mechanisms and Co-Occurrence Patterns of Protistan-Bacterial Microbiotas in the Western Pacific Ocean. *mSystems* 8, e0001323.

Sutton, T. T. (2013). Vertical ecology of the pelagic ocean: classical patterns and new perspectives. *J. Fish Biol.* 83, 1508–1527.

Sutton, T. T., Clark, M. R., Dunn, D. C., Halpin, P. N., Rogers, A. D., Guinotte, J., et al. (2017). A global biogeographic classification of the mesopelagic zone. *Deep Sea Res. Part I* 126, 85–102.

Sutton, T. T., Porteiro, F. M., Heino, M., Byrkjedal, I., Langhelle, G., Anderson, C. I. H., et al. (2008). Vertical structure, biomass and topographic association of deep-pelagic fishes in relation to a mid-ocean ridge system. *Deep Sea Res. Part 2 Top. Stud. Oceanogr.* 55, 161–184.

Thibault, H., Ménard, F., Abitbol-Spangaro, J., Poggiale, J.-C., and Martini, S. (2025). Modeling the contribution of micronekton diel vertical migrations to carbon export in the mesopelagic zone. *Biogeosciences* 22, 2181–2200.

Thomsen, P. F., Jensen, M. R., and Sigsgaard, E. E. (2024). A vision for global eDNA-based monitoring in a changing world. *Cell*. doi: 10.1016/j.cell.2024.04.019

Tipton, L., Müller, C. L., Kurtz, Z. D., Huang, L., Kleerup, E., Morris, A., et al. (2018). Fungi stabilize connectivity in the lung and skin microbial ecosystems. *Microbiome* 6, 12.

Tolochko, P., and Vadrot, A. B. M. (2021). The usual suspects? Distribution of collaboration capital in marine biodiversity research. *Mar. Policy* 124, 104318.

Travis, J. M. J., Brooker, R. W., and Dytham, C. (2005). The interplay of positive and negative species interactions across an environmental gradient: insights from an individual-based simulation model. *Biol. Lett.* 1, 5–8.

Tyner, S., Briatte, F., and Hofmann, H. (2017). Network visualization with ggplot2. *R J.* 9, 27.

Webb, T. J., Vanden Berghe, E., and O'Dor, R. (2010). Biodiversity's big wet secret: the global distribution of marine biological records reveals chronic under-exploration of the deep pelagic ocean. *PLoS One* 5, e10223.

Wickham, H. (2016). *Ggplot2: Elegant graphics for data analysis*., 2nd Edn. Cham, Switzerland: Springer International Publishing.

Wiebe, P. H., Madin, L. P., Haury, L. R., Harbison, G. R., and Philbin, L. M. (1979). Diel vertical migration bySalpa aspera and its potential for large-scale particulate organic matter transport to the deep-sea. *Mar. Biol.* 53, 249–255.

Willis, C., Gardner, K. G., Arostegui, M. C., Braun, C. D., Golet, W., Houghton, L., et al. (2025). Evaluating the importance of mesopelagic prey to three top teleost predators in the northwest Atlantic Ocean. *ICES J. Mar. Sci.* 82, fsaf028.

Xiao, Y., Angulo, M. T., Friedman, J., Waldor, M. K., Weiss, S. T., and Liu, Y.-Y. (2017). Mapping the ecological networks of microbial communities. *Nat. Commun.* 8, 2042.

Yang, N., Jin, D., and Govindarajan, A. F. (2024). Applying environmental DNA approaches to inform marine biodiversity conservation: The case of the Ocean Twilight Zone. *Mar. Policy* 165, 106151.

Yates, M. C., Derry, A. M., and Cristescu, M. E. (2021). Environmental RNA: A Revolution in Ecological Resolution? *Trends Ecol. Evol.* 36, 601–609.

Yeh, Y.-C., and Fuhrman, J. A. (2022). Contrasting diversity patterns of prokaryotes and protists over time and depth at the San-Pedro Ocean Time series. *ISME Communications* 2, 1–12.

Zeldis, J. R., Davis, C. S., James, M. R., Ballara, S. L., Booth, W. E., and Chang, F. H. (1995). Salp grazing:effects on phytoplankton abundance, vertical distribution and taxonomic composition in a coastal habitat. *Mar. Ecol. Prog. Ser.* 126, 267–283.

Zhang, G. K., Chain, F. J. J., Abbott, C. L., and Cristescu, M. E. (2018). Metabarcoding using multiplexed markers increases species detection in complex zooplankton communities. *Evol. Appl.* 11, 1901–1914.

9. Data accessibility statement

All relevant data, metadata, and code used in this study are available openly available on GitHub at https://github.com/yang-nina/OTZ-AR43-Metabarcoding. Raw sequence reads are deposited in the SRA (BioProject accession PRJNA1454214).

10. Benefit-sharing statement

Benefits of this research are shared as all relevant data, results, and code necessary to reproduce this study.

11. Conflict of interest disclosure

The authors report no conflicts of interest.